Ruthenium(II) complexes with phosphonate-substituted phenanthroline ligands as reusable photoredox catalysts

Gleb Morozkov, Anton Abel, Konstantin Lyssenko, Vitaly Roznyatovsky, Alexei Averin, Irina Beletskaya, Alla G. Bessmertnykh-Lemeune

Ruthenium(II) complexes with phosphonate-substituted phenanthroline ligands as reusable photoredox catalysts

Gleb V. Morozkov,[a] Anton S. Abel,*[a] Konstantin A. Lyssenko,[a,b] Vitaly A. Roznyatovsky,[a] Alexei D. Averin,[a] Irina P. Beletskaya,[a,c] and Alla Bessmertnykh-Lemeune*[d]

[a] *Lomonosov Moscow State University, Department of Chemistry, 1-3, Leninskie Gory, Moscow, 119991, Russia*

[b] *National Research University Higher School of Economics, Miasnitskaya Str. 20, 101000, Moscow, Russian Federation*

[c] *Frumkin Institute of Physical Chemistry and Electrochemistry, Russian Academy of Sciences, Leninsky Pr. 31, Moscow 119071, Russian Federation*

[d] *ENS de Lyon, UMR 5182, CNRS, Laboratoire de Chimie, 69342 Lyon, France*

ABSTRACT: Ru(II) complexes with polypyridyl ligands (2,2´-bipyridine = bpy, 1,10-phenanthroline = phen) play a central role in the development of photocatalytic organic reactions. In this work, we synthesized four mixed-ligand $[Ru(phen)(bpy)_2]^{2+}$-type complexes (**Ru-Pcat-A**) bearing two phosphonate substituents P(O)(OH)(OR) (R = H, Et) attached to the phen core at positions 3,8- (**Ru-3,8PH** and **Ru-3,8PHEt**) and 4,7- (**Ru-4,7PH** and **Ru-4,7PHEt**) of the heterocycle in high yields (87–99%) and characterized them using spectral methods. Single crystal X-ray diffraction was employed to determine the coordination mode of the ditopic phen ligand in **Ru-4,7PH**. This complex exists as the neutral species and forms a the 1D hydrogen-bonded framework in the crystals. The light absorption characteristics were found to be similar for all complexes prepared in this work. However, the emission maxima in aqueous solutions were significantly affected by the substitution of the heterocycle, ranging from 629 nm for **Ru-4,7PH** to 661 nm for **Ru-3,8PHEt**. The emission quantum yields in Ar-saturated deionized water showed strong dependency on the substitution pattern of the phen ligand, with maximal values reaching approximately 0.11 for **Ru-4,7PHEt** and **Ru-4,7PH**, which is twice as high as that of the classical $[Ru(bpy)_3]^{2+}$ complex (**Ru-bpy**). Photocatalytic performance of **Ru-Pcat-A** was investigated using visible light photoredox catalytic transformations of tertiary amines. With **Ru-Pcat-A**, we achieved the phosphonylation of *N*-aryl-1,2,3,4-tetrahydroisoquinolines (THIQs) and cyanation of THIQs and *N*,*N*-dimethylaniline in methanol, while a mixture of nitromethane/methanol (1:1 v/v) proved to be the optimal solvent for conducting the nitromethylation of THIQs. In the

majority of the studied reactions, **Ru-4,7PHEt** exhibited greater efficiency compared to **Ru-bpy**, and it could be easily separated from the products using water extraction and reused in the next catalytic cycle. We successfully performed seven consecutive nitromethylation and phosphorylation of *N*-phenyl-1,2,3,4-tetrahydroisoquinoline using the recycled homogeneous photoredox catalyst.

INTRODUCTION

Visible light-active Ru(II) and Ir(III) complexes incorporating chelating ligands with pyridyl residues such as 2,2´-bipyridine (bpy) and 1,10-phenanthroline (phen) have been extensively studied in molecular electronics, biomolecule labeling, development of solar fuels production and functional supramolecular systems, and electro- and photocatalysis.[1–3] In organic synthesis, these complexes have been widely explored as photosensitizers in the aerobic oxidation reactions.[4,5] Recent studies have focused on their key role in visible-light photoredox catalysis.[6–10] These reactions have gained enormous interest during the last two decades as they enable unusual synthetic strategies for the preparation of complex organic compounds containing various functional groups, while also addressing the growing demand for renewable energy usage.[5,11,12] Remarkable photostability of these complexes and their exceptional photophysical and redox properties[13,14] have made them highly demanded in this rapidly developing field.[15] However, despite these advantages, the high cost, toxicity and reliance on non-abundant metals present serious limitations for their use in industrial production of fine chemicals. Therefore, significant research efforts are directed towards developing recoverable Ru(II) and Ir(III)-based photocatalytic systems.[16] While heterogenization techniques have been extensively studied, photocatalyst (PC) recycling through liquid phase-separation processes offers distinct advantages in terms of avoiding slow mass diffusion phenomena, optimizing light utilization, and facilitating adaptability to flow conditions. Surprisingly, the development of Ru(II) complexes for such processes has predominantly focused on derivatives with long alkyl chains, soluble in non-polar media.[16] Water-soluble complexes have received less attention, likely due to the influence of counter-ions on the solubility of Ru(II) complexes in water and polar organic solvents. The exchange of labile counter-ions during photocatalytic transformations may potentially affect their solubility and recycling process.

In our research, we are investigating metal complexes with phenanthroline ligands which can be used as reusable catalysts.[17] 1,10-Phenanthroline, compared to bipyridine, is structurally preorganized for metal chelation and is expected to yield more stable complexes.[18–20] Additionally, phenanthroline can be easily functionalized using various synthetic strategies.[21] Directed functionalization of this azaheterocycle can be used for fine tuning the solubility and photophysical properties of the resulting complexes, for their immobilization on solid supports, and in the development of bimetallic catalytic systems involving two different catalytic centers. While the photophysical properties of ruthenium complexes with bpy and phen ligands are often comparable, the latter ligand has been rarely utilized in photocatalysis and only homoleptic complex $[Ru(phen)_3]X_2$ (X = Cl, PF_6) was explored in photocatalytic transformations.[22–26]

Recently, we have shown that Ru(II) complexes bearing diethoxyphosphoryl ($P(O)(OEt)_2$)-substituted phen ligands (**Ru-4,7PEt** and **Ru-3,8PEt** (Figure 1), for instance) are valuable catalysts for homogeneous photoreactions.[27] These complexes exhibit high solubility in various organic solvents, high brightness, and variable redox potentials that influence the rate and selectivity of photocatalytic reactions. For example, **Ru-4,7PEt** is more efficient than **Ru-bpy** in the photocatalytic oxidation of sulfide to sulfoxides by molecular oxygen which mainly proceeds through an energy transfer mechanism and involves the generation of singlet oxygen. Additionally, we have prepared a mixed-ligand complex [Ru(**phen-C**)$(bpy)_2$]Cl_2 containing bpy and 1,10-phenanthroline-3,8-dicarboxylic acid (**phen-C**) ligand.[28] This complex has been successfully used as a reusable catalyst in photocatalytic aerobic oxidation of sulfide to sulfoxides.

In this work, we have developed synthetic approaches to Ru(II) complexes with phen ligands bearing phosphonic acid and their monoethyl esters (**Ru-Pcat-A**) shown in Figure 1. This structural modification allows for fine-tuning the hydrophilic-lipophilic balance (HLB) of complexes, which is crucial for their solubility and the development of PC recycling. Our synthetic approach enables efficient synthesis of isomeric bis(phosphonate)-substituted complexes in excellent yields (87–99%) without employing any toxic or expensive reagents. All complexes obtained were characterized by spectral methods. Single crystal X-ray diffraction was also used to investigate **Ru-4,7PH** in the solid state. Complexes **Ru-Pcat-A** are emissive, and derivatives with phosphonate groups located at positions 4 and 7 demonstrate remarkable brightness in Ar-saturated aqueous solutions. The photocatalytic

performance of **Ru-Pcat-A** in photoredox catalytic transformations of *N*-aryl-1,2,3,4-tetrahydroisoquinolines (THIQs) was investigated, and their reusability was shown.

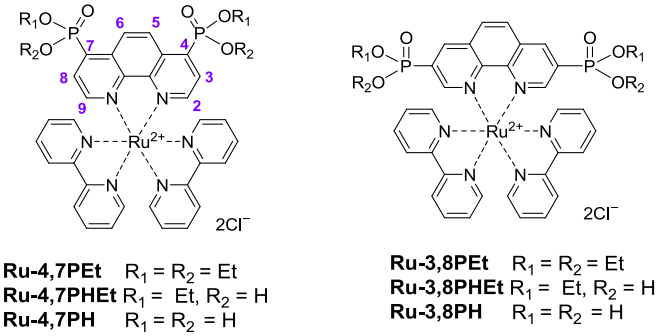

Figure 1. Structures of investigated phosphonate-substituted Ru(II) complexes **Ru-Pcat-A** and related compounds **Ru-4,7PEt** and **Ru-3,8PEt** reported by us previously.[27]

RESULTS AND DISCUSSION

Synthesis

$[Ru(bpy)_3]^{2+}$-type complexes with 2,2'-bipyridines bearing phosphonic acid groups has been reported for the first time more than twenty years ago,[29] and their synthesis has been carefully optimized due to wide range of their applications.[18–20,30–43] Despite several synthetic strategies were explored to prepare these compounds,[31,44,45] it was found that only treating Ru(II) complexes with diethyl phosphonate substituents with an excess of the expensive and irritant Me_3SiBr, followed by the addition of methanol, afforded corresponding acids in high yields (up to 90–96%).[20,29,43,46,47] In our preliminary experiments, we relied on these data to prepare complexes **Ru-Pcat-A**.

Therefore, we opted to synthesize them from complexes **Ru-3,8PEt** and **Ru-4,7PEt** as shown in Scheme 1 (pathways (*ii*) and (*iii*)). **Ru-3,8PEt** was treated with an excess of Me_3SiBr in acetonitrile, followed by the addition of methanol. This reaction sequence afforded the desired product in 80% yield, as confirmed by ^1H NMR analysis of the reaction mixture. However, our attempts to isolate the product through precipitation by various organic solvents were unsuccessful, highlighting the indispensability of the size exclusion chromatography in post-synthetic treatment.

On the other hand, performing the synthesis of **Ru-3,8PEt** and **Ru-4,7PEt**, we obtained partially hydrolyzed products as main side products (see ESI, section 3 and

Figures S47-S50, S59 and S60). This side reaction had already been observed in the synthesis of $P(O)(OEt)_2$-substituted $[Ru(bpy)_3]^{2+}$-type complexes.[48–51] We hypothesized that phen derivatives **Ru-3,8PEt** and **Ru-4,7PEt** could be easily hydrolyzed in aqueous media and investigated this synthetic strategy to prepare **Ru-Pcat-A**. Indeed, **Ru-4,7PEt** was completely consumed in boiling EtOH/water solvent mixture in the presence of hydrochloric acid or sodium hydroxide (Table S1). However, we were unable to purify the product. Fortunately, when the reaction temperature was increased to 150 °C, the hydrolysis proceeded smoothly without any catalyst and pure complexes **Ru-4,7PH** and **Ru-3,8PH** were obtained by simply evaporating the reaction mixture under reduced pressure. These findings allowed us to optimize the two-step synthesis shown in Scheme 1, performing the hydrolysis of the crude mixture of complexes with chloride counter-ions obtained in the first step (Table S1). By conducting the synthesis in this way, the analytically pure complexes **Ru-4,7PH** and **Ru-3,8PH** were obtained in their protonated forms $[Ru(bpy)_2(4,7\text{-}PH)](Cl)_2$ (4,7-PH = 1,10-phenanthroline-4,7-diphosphonic acid) and $[Ru(bpy)_2(3,8\text{-}PH)](Cl)_2$ (3,8-PH = 1,10-phenanthroline-3,8-diphosphonic acid) in overall yields of 94% and 87%, respectively. Noteworthy, these yields are higher compared to those observed in the synthesis of **Ru-4,7PEt** and **Ru-3,8PEt** (Scheme 1, pathway (*i*)) because partially hydrolyzed side products were also transformed in the target products **Ru-4,7PH** and **Ru-3,8PH.**

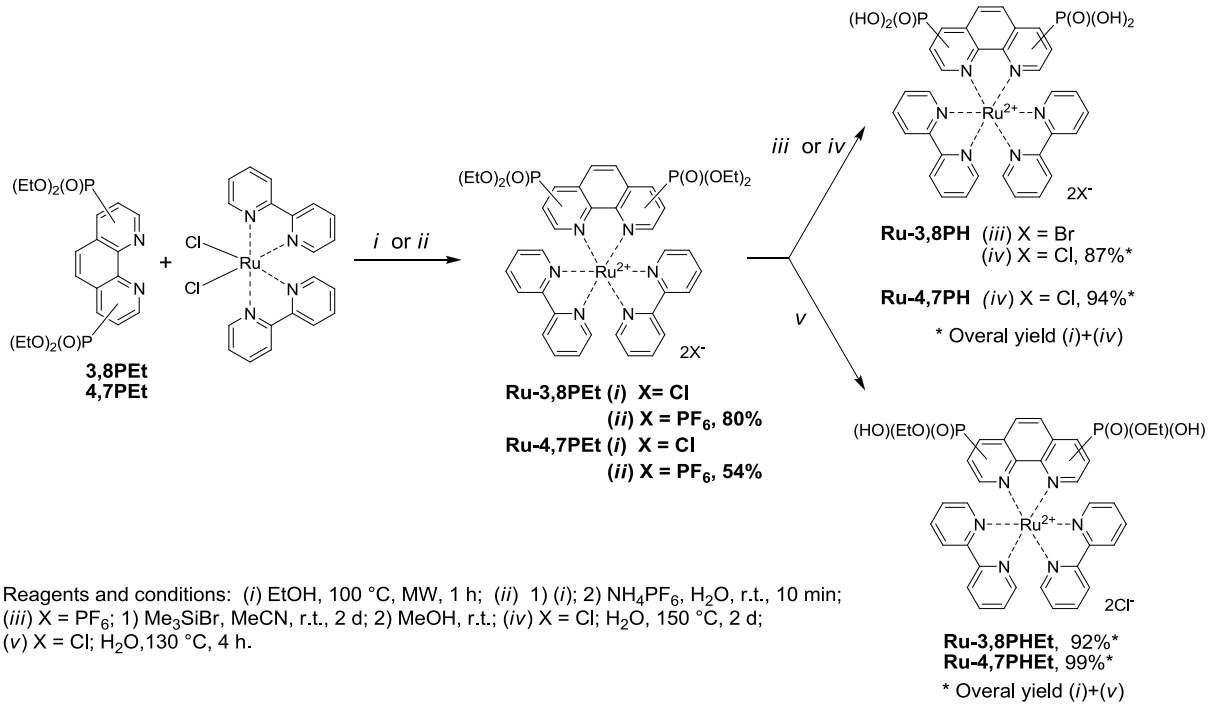

Scheme 1. Synthesis of phosphonate-substituted complexes **Ru-3,8PHEt**, **Ru-4,7PHEt**, **Ru-3,8PH** and **Ru-4,7PH**.

Interestingly, by decreasing the reaction temperature to 130 °C, we obtained selectively **Ru-3,8PHEt** and **Ru-4,7PHEt** in 99% and 92% yields, respectively, using the same very easy post-synthetic treatment (Scheme 1). The high selectivity in this reaction is not entirely surprising, as the selective hydrolysis phosphonate diesters to monoesters was reported and can be achieved through their refluxing in polar organic solvents in the presence of aqueous NaOH.[52] However, to the best of our knowledge, the reaction reported here is the first example in which heteroaromatic phosphonates monoesters have been successfully prepared in water without adding bases. Noteworthy, Ru(II) complexes with bipyridine ligands bearing P(O)(OH)(OEt) groups were prepared only occasionally and their properties are still scarcely investigated.[48,49]

The purity of complexes **Ru-Pcat-A** being synthesized was evidenced by mass spectrometry and NMR spectroscopy (Figures S39–S46, S51–S58). The successful transformations of phen ligand were confirmed by observation of $[M–Cl]^+$ ion peak with matching isotopic pattern as the most prominent peak in the high resolution mass spectra (Figures S55–58). Complexes **Ru-Pcat-A** were found to be soluble in methanol, ethanol, DMF, DMSO, and aqueous media and showed high photostability as was proved by irradiating their solutions in water, MeOH and DMSO with blue LED for 48 h (Figure S1). Such high photostability of **Ru-Pcat-A** can be expected

considering the enhanced photostability of previously reported Ru(II) complexes with electron-withdrawing substituents in bpy ligands.[53] Using the developed reaction conditions, we also attempted to improve the synthesis of 1,10-phenanthrolines bearing phosphonic acid residues (Table S2). Unfortunately, the hydrolysis of dialkyl phosphonate **4,7PEt** in water at 150 °C proceeded so slowly that these experimental conditions cannot be considered as an improvement over the known methods.

Despite the limitations in scope, our experimental conditions hold practical interest due to the extensive study of Ru(II) complexes with phosphonate-substituted polypyridyl residues. Their usual large-scale preparation poses challenges as it requires a large excess of Me_3SiBr and involves size exclusion chromatography.

Insights in the solid state structure of Ru-4,7PH

Phosphonic acid groups of polypyridine ligands can ligate to the ruthenium ions, but only when they are positioned adjacent (α-) to the nitrogen atom allowing them to participate in the formation of the chelate cycle.[54] In all other Ru(II) complexes, including $[Ru(bpy)_2(bpy\text{-}P)]^{2+}$-type (bpy-P = phosphonate-substituted bpy) complexes, the phosphonate group attached directly to the phen core does not coordinate to the metal ions.[27] Our attempts to grow single crystals of complexes **Ru-Pcat-A** only resulted in good-quality crystals of **Ru-4,7PH**. The crystal structure of **Ru-4,7PH** was authenticated by single-crystal X-ray diffraction analysis. Overall, the geometry of this complex is rather similar to that of previously reported **Ru-4,7PEt**, and the phosphonate groups are non-coordinated in both structures.[27] The six-coordinated ruthenium center is chelated by nitrogen atoms from two bpy ligands and one phen ligand bearing phosphonate groups, and adopts a slightly distorted octahedral geometry (Figure 2). All metal–nitrogen bond lengths (Ru–N = 2.041(3)-2.062(3)Å) lay and vary in the expected range[27,55–57] and are almost insensitive to the presence of the phosphorus substituents, regardless of the substituents (H or Et) present on the phosphonate groups.

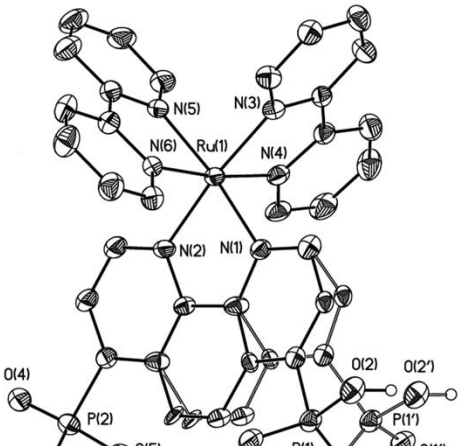

Figure 2. Structure of ~~cationic~~ complex **Ru-4,7PH**. Outer sphere counter ions, hydrogen atoms and solvent molecules are omitted for clarity. Selected bond lengths (Å): Ru–N(1–6) = 2.051(3)–2.062(3); P(1)–O(3) 1.44(6), P(1)–O(1) 1.480(8), P(1) O(2) 1.568(6), P(1)–C(3) 1.815(8), P(1')–O(3') 1.48(4), P(1')–O(1') 1.487(6), P(1')–O(2') 1.563(6), P(1')–C(3') 1.48(4), 1.811(8).

It should be noted that one phosphonate group is disordered over two positions. The bond lengths within such groups are of great importance considering that the degree of their protonation determine the overall charge of the complex. The ordered phosphonate group is clearly monodeprotonated with two relatively short 1.487(3) and 1.518(3) P–O bonds, and one longer bond at 1.566(3). This conclusion is consistent with the hydrogen atom position location and with the H-bond pattern observed for $P(2)O_3H$ group. Indeed, the latter forms the centrosymmetric hydrogen-bonded P(1)–O(5)-H(5)…O(6) (O…O 2.559(6) Å, OHO 161 °) dimer (Figure 3). Assuming the strengths of this hydrogen bond, the slight elongation of P(2) –O(4) bond seems rather reasonable. The analysis of bond lengths for the second group should be addressed with caution due to the presence of disorder, but the geometry of these fragments turned out to be virtually identical, given the absence restraints and constraints on the refinement. Moreover, the analysis of crystal packing has revealed that each of equally occupied positions (**A**, **B**), of disordered group is involved in the same hydrogen-bonded assembly as P(2)group. Interestingly, the OH group of position **A** interacts with P=O group of **B** while OH group of **B** interacts with P=O group of **A**. As a result, dianions are interconnected into the hydrogen-bonded zig-zag chain along crystallographic axis c (Figure 3), in which the neighboring molecular fragments have alternate positions of disordered P(1`) group. Finally, we can conclude that ruthenium complex in crystal exist in the neutral form and ~~and~~ forms a 1D hydrogen bond framework. Nevertheless, the presence of an uncoordinated chloride anion has been established, indicating the necessity of another cation in the structure. The analysis of hydrogen bonds and electron density difference synthesis allowed to localize the mentioned oxonium ion (Figure S2). The latter are involved with chloride anion and

solvate water molecules into infinite chains directed along crystallographic axis b ~~(Figure S3)~~.

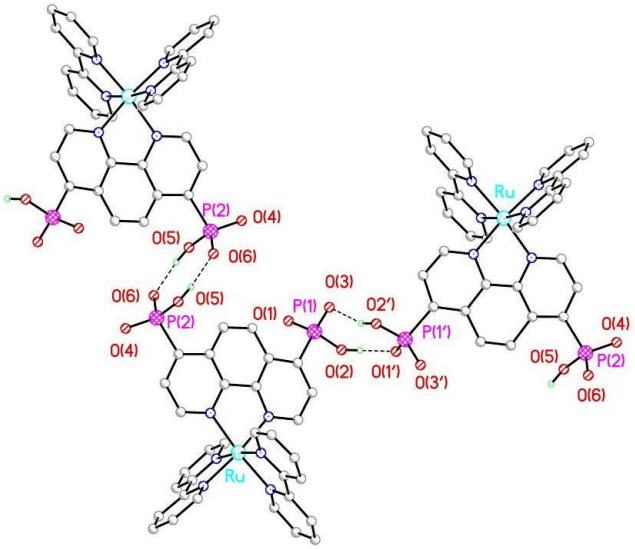

Figure 3. 1D hydrogen-bonded framework formed in crystals of **4,7RuPH**.

Characterization in solution by NMR spectroscopy

Solution structures and kinetic inertness of all studied complexes were confirmed by NMR spectroscopy. The ^{1}H NMR spectrum of representative complex **Ru-4,7PH** is shown in Figure 4, and other spectra (^{1}H, ^{31}P and ^{13}C and so forth) are collected in ESI (Figures S4–S11, S43, and S44).

As shown in Figure 4, the ^{1}H NMR spectra of **Ru-4,7PH** is typical spectra of $[Ru(bpy)_2(phen)]^{2+}$ chelates having D_3 symmetry. Comparing ^{1}H and ^{31}P chemical shifts of phosphonate substituents in reported compounds and our complexes **Ru-Pcat-A** we assumed that phosponate groups remain uncoordinated in these complexes. For instance, characteristic signals of OCH_2 group protons in P(O)(OEt)(OH) substituents appear as multiplets δ_H 3.77–3.84 and 3.50–3.56 ppm in **Ru-4,7PHEt** and **Ru-3,8PHEt**, respectively. These δ_H values are rather similar to those observed in other compounds with non-coordinated ethyl phosphonate groups P(O)(OH)(OEt).[52,58]

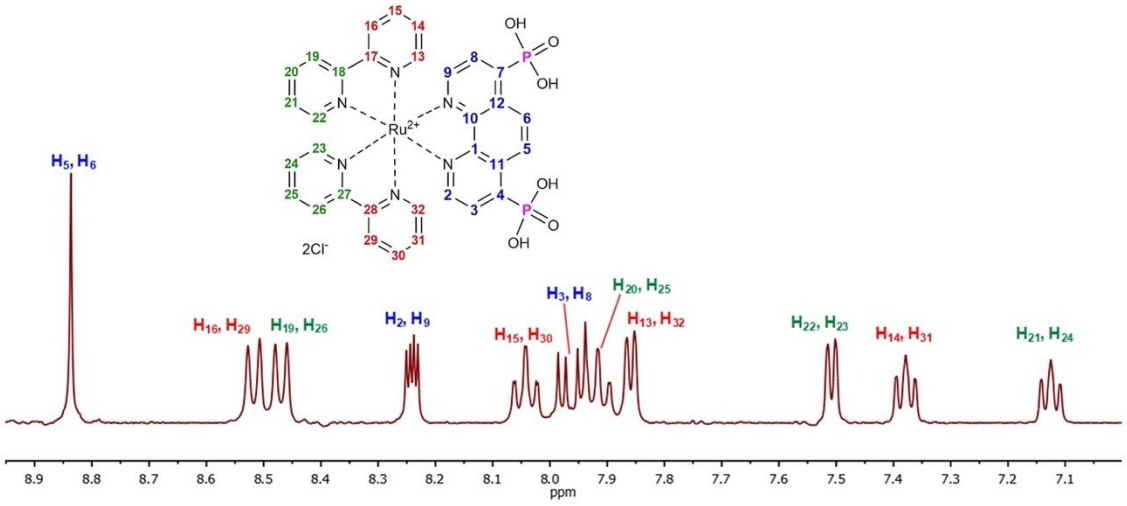

Figure 4. Selected region of ^{1}H NMR spectrum of **Ru-4,7PH** in D_2O at room temperature.

All proton signals of the phen ligand were easily assigned based on the values of chemical shifts and coupling constants, which are typical for 4,7-diphosphonate-substituted phenanthrolines ($^{3}J_{H,H}$ = 5.3 Hz, $^{3}J_{H,P}$ = 12.8 Hz, $^{4}J_{H,P}$ = 2.2 Hz) (Table S6).[27] The remaining signals comprise two sets, each composed of two doublets, and two triplets. This pattern is expected for bpy ligands because two pyridine residues of each bpy ligand have different environments. Despite ^{13}C NMR spectra being complicated and less convenient for structural analysis, ^{1}H–^{13}C HMBC experiments provide crucial information on the connectivity of py residues due to the presence the cross-peaks for the C17, C18 (C27, C28) carbon nuclei and H19, H16 (H26, H29) protons (Figure S9). When programming the ^{1}H–^{13}C HMBC experimental parameters, particular attention should be paid to the value of the coupling constant ($^{3}J_{H,H}$ = 5 Hz). HMBC experiments are known to be quite susceptible to different artifacts, which could lead to incorrect signal assignments.[27]

In the course of our previous and these studies, we synthesized a large series of $[Ru(bpy)_2(phen)]^{2+}$ complexes. Analyzing our data (Tables S3, S6–S8, Figures S3–S31), we noted several trends which are helpful for the proton assignment in complexes of $[Ru(bpy)_2(phen)]^{2+}$ series. When one bpy ligand in the complex $[Ru(bpy)_3]^{2+}$ is replaced with a phen ligand, specific shifts in the α-protons (α-H) of the bpy ligand directed towards the phen ligand (H13 and H32, Figures 4 and S3) are observed. These protons were observed to be more than δ_H 0.20 ppm downfield from those in $[Ru(bpy)_3]^{2+}$, while the analogous protons in the second py residue of the same bpy ligand experienced a small upshift (the maximal value of δ_H 0.08 ppm). Notably,

the presence of various substituents on the phen ligand did not significantly impact the chemical environment of these α-H of the distant py residues and their chemical shifts are close for all complexes investigated even when the spectra were recorded in different solvents. Moreover, the chemical shift of the δ-H of py residues located near the phen ligand did not change significantly (less than δ_H 0.06 ppm), regardless of the type and position of the substituent attached to the phen ring (Tables S3 and S4).

Based on these data, complete proton assignment in the $[Ru(bpy)_2(phen)]^{2+}$-type complexes with two unsubstituted bpy ligands and the symmetrical disubstituted phen ligand can be achieved using only ^1H and COSY (or TOCSY) experiments without the need for employing ^1H–^{13}C HMBC experiments (Table S4). The analysis of the spectrum should begin with the attribution of α-H signals, which have chemical shifts very close to those observed in the parent $[Ru(bpy)_3]^{2+}$ complex (δ_H 7.73 ppm). By using data from COSY or TOCSY experiments, all protons of two py residues bearing these α- protons can be identified. The signals with chemical shifts very similar to those of the β (H21)-, γ (H20)-, and ω (H19)-protons of these rings correspond to their analogous protons (H14, H15, and H16, respectively) in the other py residues. The remaining proton correlated with the β (H14)- protons in the COSY experiments represents the α-H of these py residues and directed towards the phen ligand (H13 and H32). The assignment of the remaining protons of the phen ligand can generally also be performed using the COSY spectrum.

Unfortunately, this comparative analysis of proton chemical shifts does not allow for the complete assignment of signals in the ^1H NMR spectra of complexes $[Ru(bpy)_2(phen)]^{2+}$-type with asymmetric phen ligands. Further detailed discussion on this matter is provided in ESI (section 6, Table S5).

Photophysical properties

The electronic absorption and emission spectra of newly synthesized **Ru-Pcat-A** complexes were recorded in water at room temperature (Figure 5 and S38). The data obtained in these studies are summarized in Table 1.

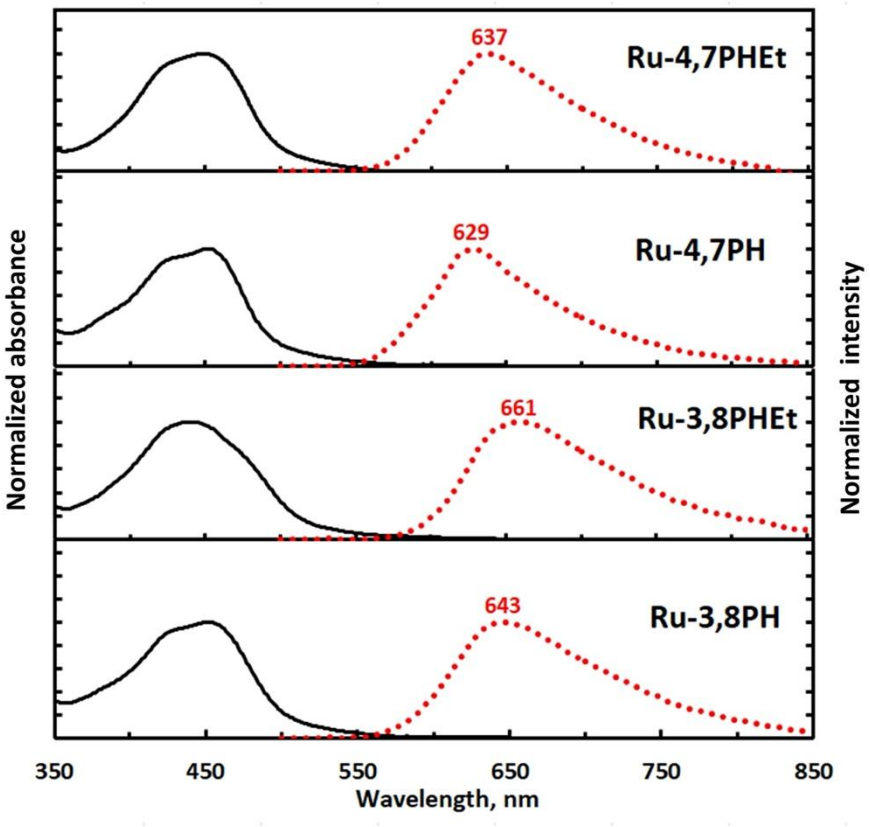

Figure 5. Absorption (black solid line) and emission (red dotted line) spectra of **Ru-Pcat-A** complexes in aqueous solution at room temperature.

The shape of the absorption bands of **Ru-bpy** changes only slightly after the replacement of one bpy ligand with a phosphonated phen chelator. All complexes **Ru-Pcat-A** exhibit intense absorption bands in the 250–350 nm region, which are generally assigned to ligand-centered π–π* electronic transitions.[61] Absorption bands in the longer wavelength region (400–500 nm) are broadened due to the overlapping spin-allowed metal-to-ligand charge transfer (MLCT) and interligand bpy–phen-based charge transfer (LLCT) transitions. The positions of the absorption maxima for **Ru-Pcat-A** are relatively insensitive to the substitution pattern at the phen ligand and the degree of hydrolysis of phosphonate groups. However, the intensity of absorption of 4,7-disubstituted complexes **Ru-4,7PHEt** and **Ru-4,7PH** is higher compared to that of their isomers **Ru-3,8PHEt** and **Ru-3,8PH**, in particular in the working region of blue LED (430–480 nm).

As shown in Table 1, the complexes exhibit luminescence emission in water at room temperature, which is strongly quenched in the presence of oxygen, as is also observed for **Ru-bpy.**[60] The replacement of bpy ligand by phen with phosphonate

groups resulted in a red shift (11–33 nm (909091–303030 cm^{-1})) of the emission maxima for all complexes except **Ru-4,7PH**. Such emission red shift is commonly observed for Ru(II) complexes with ligands bearing electron-withdrawing substituents.[53] Interestingly, quantum yields (λ_{em}) in Ar-saturated deionized water were independent on the degree of hydrolysis of phosphonate groups but were found to be significantly different for isomeric complexes. The complexes with phosphonate groups at position 3 (**Ru-3,8PHEt** and **Ru-3,8PH**) were less emissive than **Ru-bpy**. They displayed an intensity of emission comparable to that of previously reported Ru(II) complexes with other $P(O)(OH)_2$-substituted polypyridine ligands (0.02-0.04).[41] In contrast, Φ_{em} reached approximately 0.11 in the case of **Ru-4,7PHEt** and **Ru-4,7PH**. This value is twice as high as that of the classical photoredox catalyst **Ru-bpy** in deaerated aqueous solution.

The apparent Stokes shifts for the studied complexes are slightly larger than that of the parent **Ru-bpy** (56818 cm^{-1}), and they are increased in the following order: **Ru-4,7PHEt** (55865 cm^{-1}) < **Ru-4,7PPH** (53475 cm^{-1}) < **Ru-3,8PH** (52083 cm^{-1}). The maximal value (45454 cm^{-1}) was observed for the **Ru-3,8PHEt** complex. It is noteworthy that the same trend was observed for analogous diester-substituted derivatives **Ru-3,8PEt** and **Ru-4,7PEt**, which were investigated in acetonitrile solution.[27]

Based on the data obtained from these studies, it appears that complexes **Ru-Pcat-A** show promise as photoredox catalysts. In particular, **Ru-4,7PHEt**, exhibiting a higher brightness than classical **Ru-bpy**, seems to be of interest for photocatalytic applications. However, the limited solubility of **Ru-Pcat-A** in polar aprotic organic solvents like acetonitrile could hinder their usefulness in organic synthesis.

Photocatalytic properties

The last two decades have witnessed an exponentially increased interest in photoredox-catalyzed reactions proceeding under visible light irradiation.[7,9,10] These transformations, which involve a single electron transfer processes provide many new synthetic tools for the preparation of organic compounds. Moreover, these reactions often occur under mild conditions, making them convenient for the synthesis of compounds containing several chemically sensitive functional groups.

Table 1. Selected photophysical parameters for **Ru-bpy** and **Ru-Pcat-A** complexes.

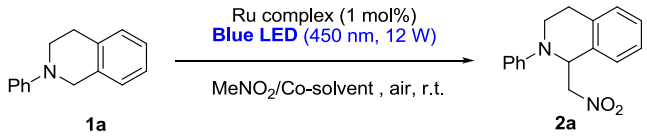

Compound	Solvent	λ_{abs} (nm) ($\varepsilon \times 10^{-3}$ (M^{-1} cm^{-1}))	λ_{em} (nm)[a]	Φ_{em}[b]	Reference
Ru-bpy	H_2O	452 (14.0), 286 (8.14), 243 (2.55)	628	0.063	[59,60]
Ru-4,7PEt	MeCN	445 (17.4), 261(85.0)	651	0.101[c]	[27]
Ru-4,7PHEt	H_2O	450 (18.2), 278 (79.2)	637	0.112	this work
Ru-4,7PH	H_2O	450 (17.3), 282 (68.1), 274 (69.6)	629	0.115	this work
Ru-3,8PEt	MeCN	481 (6.8), 435 (10.2), 284 (52.0), 272 (62.0)	697	0.021[c]	[27]
Ru-3,8PHEt	H_2O	441 (12.9), 284 (66.5), 271 (79.2)	661	0.023	this work
Ru-3,8PH	H_2O	451 (12.3), 284 (60.7), 270 (66.5)	643	0.030	this work

[a] Emission was excited at 450 nm. [b] Measured in Ar-saturated solvent relative to a solution of **Ru-bpy** in acetonitrile as a standard.[60] [c] Measured in deaerated acetonitrile at ambient temperatures relative a solution of **Ru-bpy** in acetonitrile as a standard.[27]

C–H functionalization reactions, which are known as cost-effective and powerful methods of organic synthesis,[62] can also benefit from visible light photoredox catalysis.[63] Among these reactions, the oxidative functionalization of C–H bonds adjacent to a nitrogen atom plays a crucial role because these structural residues are commonly found in compounds that are increasingly targeted in medicinal and organic chemistry.[64] The possible mechanism of the visible light photoredox-catalyzed oxidative coupling of tertiary amines with nucleophiles in air is shown in Scheme 2.[65]

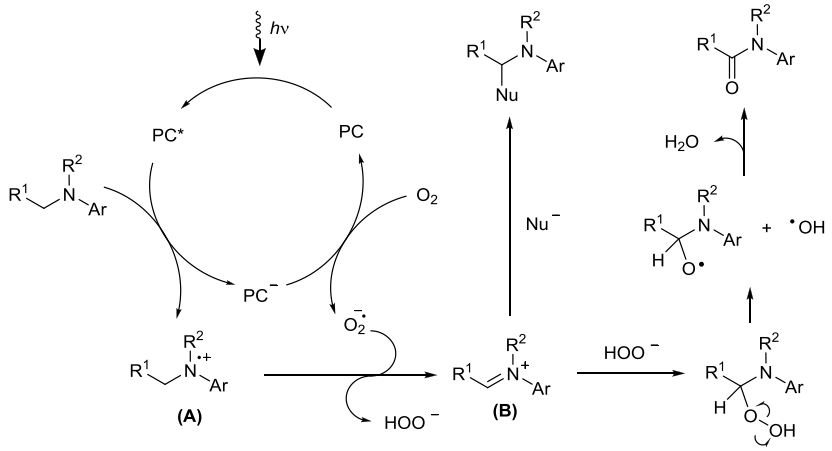

Scheme 2. Transformations involved in α-functionalization of tertiary amines by nucleophiles under visible light irradiation in air.

The excited photocatalyst (PC*) here would rather oxidize the electron-rich amine donor to further pass the electron to oxygen molecule generating superoxide ($O_2 \cdot^-$). These species can be transformed to iminium cations which may then capture nucleophiles to give *α*–functionalized amines as in the case of Mannich-type reactions. Under appropriate reaction conditions, this photocatalytic reaction smoothly proceed with a wide range of nucleophiles such as nitromethane, dialkyl *H*-phosphonates, potassium cyanide, enol silanes, ketones, copper acetylides and so forth.[8] However, these transformations often afford the desired product in satisfactory yields only for *N*-aryl-1,2,3,4-tetrahydroisoquinolines (THIQs), and they are difficult to generalize for other tertiary amines.[8,66] Many undesired processes were observed in these reactions likely because superoxide anion formed in the photoredox catalytic cycle is a strong oxidant. For instance, superoxide can participate in the oxygenation of carbon atom adjacent to nitrogen atom affording amides as shown in Scheme 2. It is also noteworthy that in these reactions more expensive and generally heteroleptic Ir(III) complexes are generally more efficient than the classical **Ru-bpy**.

We selected these transformations as model reactions because each of them requires specific nucleophiles and solvents. This offers an excellent opportunity to demonstrate the photocatalytic usefulness of **Ru-Pcat-A**, as the conditions for each reported reaction had to be adjusted to the solubility of **Ru-Pcat-A**, making catalytic activity prediction *a priori* very difficult.

First, we explored **Ru-Pcat-A** in the *α*-functionalization of THIQ by nitromethane (aza-Henry reaction) (Table 2, Figure S33). The nitromethylation of THIQs[67] has been extensively used as a model reaction in comparative studies of new homogeneous and heterogeneous photoredox catalysts.[16] In these studies, nitromethane was commonly used as both a reagent and a solvent. However, solubility of **Ru-Pcat-A** complexes in nitromethane was low, which is probably why the reaction rate decreased when **Ru-bpy** was replaced by **Ru-4,7PHEt** in the nitromethylation of **1a** (entries 1 and 2).

To overcome this drawback, alcohols were added in the reaction as co-solvents. The homogenization of the reaction mixture could be achieved by adding only 3 vol% of HFIP. Under these conditions, the reaction with **Ru-4,7PHEt** proceeded as rapidly as with **Ru-bpy**, albeit with slightly lower product yield (entry 3). The desirable product was also obtained in methanol, which is less expensive than HFIP, but when

its amount was increased up to 40 vol% (entries 4–7). After 10 h of irradiation, the conversion of **1a** was higher than 93% for all **Ru-Pcat-A** complexes except **Ru-3,8PH**. Nevertheless, the reaction selectivity varied, and the highest yield of **2a** (83%) was achieved with **Ru-4,7PHEt** (entry 4). Importantly, **Ru-4,7PHEt** provided a higher product yield compared to the classical photoredox catalyst **Ru-bpy** (73%, entry 1).

Next, the substrate scope was investigated using **Ru-4,7PHEt** as a photoredox catalyst. THIQs **1b**–**e** with electron-rich and electron-deficient *N*-aryl residues were subjected to nitromethylation (Scheme 3). To our satisfaction, for most of the amines studied, the product was obtained in good yields (70–83%), which were only slightly lower (15–20%) than those reported with Ir(III) photoredox catalysts.[67] As shown in Scheme 3, only the *para*-cyano-substituted amine **2d** bearing a strong electron-withdrawing group on the aryl residue yielded the product in a moderate yield (40%).

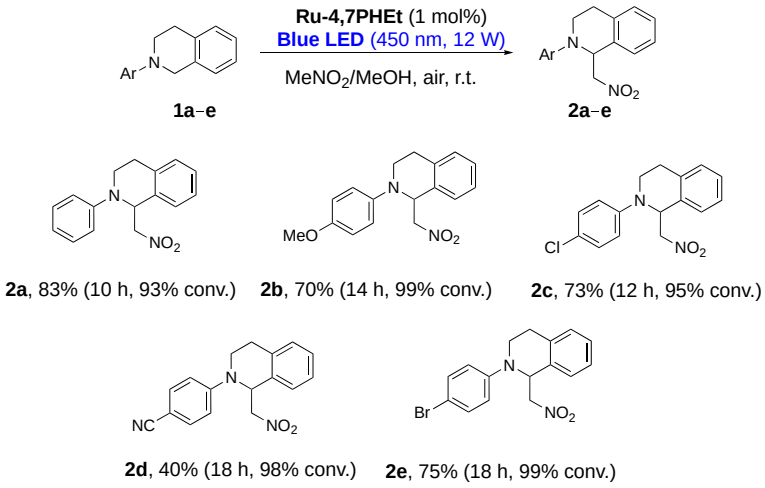

Scheme 3. Nitromethylation of *N*-aryl-1,2,3,4-tetrahydroisoquinolines **1a-e**. Reaction conditions: 1 (0.3 mmol), Ru-4,7PHEt (1 mol%), $MeNO_2$ (1.2 mL), MeOH (0.8 mL), air, blue LED (12 W), r.t. The yields and conversions were determined from NMR ^1H analysis of the reaction mixture. 1,3-Dimethoxybenzene was used as an internal standard (Figures S33 and S34).

Reactive iminium ions formed from THIQ under irradiation by blue LED in the presence of **Ru-Pcat-A** could also be involved in the C–P bond forming reactions.[68] These reactions are scarcely investigated in both homogenic and heterogenic conditions.[16] The reactions with phosphorus nucleophiles seems to be trickier compared to aza-Henry reaction probably because usually phosphorous nucleophiles are not used as solvents. Even when Ir(III) complexes, known for their excellent redox properties, used for functionalization of THIQs by dialkyl and diaryl *H*-phosphonates, the substrate scope seems to be rather limited.[68]

In our preliminary experiment, we have shown that the reaction of amine **1a** with diethyl *H*-phosphonate in the presence of **Ru-bpy** smoothly proceeded in methanol (Table 3, entry 1). Complete conversion of 1a was achieved within 6 h of irradiation, affording **3a** in 64% yield according to ^{1}H NMR analysis of the reaction mixture.

Table 3. Optimization of the photoredox-catalyzed phosphonylation reaction.[a]

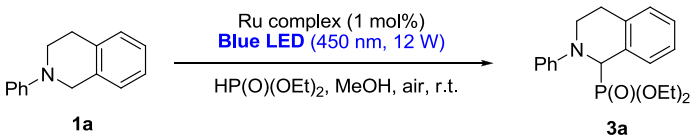

1a 3a

Entry	Ru complex	Time (h)	Conversion[b] (%)	Yield[b] (%)
1	**Ru-bpy**	6	100	64
2	**Ru-3,8PH**	4	73	61
		6	99	84
3	**Ru-4,7PH**	4	85	82
4	**Ru-3,8PHEt**	4	100	75
5	**Ru-4,7PHEt**	4	98	86

[a] Standard conditions: **1a** (78 mg, 0.375 mmol), photocatalyst (1 mol%), MeOH (1.5 mL); diethyl H-phosphonate (62 µl, 1.27 equiv, 0.488 mmol), air, blue LED (12 W), r.t. [b] The yield and conversion were determined by NMR ^{1}H analysis of reaction mixture. 1,3-Dimethoxybenzene was used as an internal standard.

The rate of this reaction in the presence of **Ru-3,8PH** was very similar, but the desired product was obtained in higher yield (84%, entry 2). The isomeric complex **Ru-4,7PH** provided an even more rapid and selective transformation of **1a** (entry 3). The (HO)(EtO)P(O)-substituted complexes **Ru-3,8PHEt** and **Ru-4,7PHEt** exhibited higher efficiency than corresponding complexes with phosphonic acid groups, with the best product yield (86%) was achieved using **Ru-4,7PHEt** (entries 4 and 5).

Encouraged by these results, we investigated the substrate scope using **Ru-4,7PHEt** as a PC (Scheme 4). Our first attempts at functionalizing THIQ **1b**, bearing an electron-rich aryl substituent, were unsuccessful due to low solubility of this amine in methanol. Additional optimization of the solvent was undertaken, and it was found that the reaction did not proceed in toluene/water and acetonitrile/water mixtures, but afforded the product in 31% yield in CH_2Cl_2/MeOH (1:1 v/v). The best product yield (50%) was obtained when CH_2Cl_2 was replaced by toluene or THF. Thus, the phospholynation of THIQs **1c** and **1d** was performed in a THF/MeOH (1:1 v/v) solvent mixture, but the products were obtained in lower yield (34%). Trifluoromethyl-substituted THIQ **1f** was soluble in MeOH, and we carried out the reaction with this electron-deficient compound in this solvent expecting increase the product yield. However, the target product **3f** was isolated once again in moderate yield (35%).

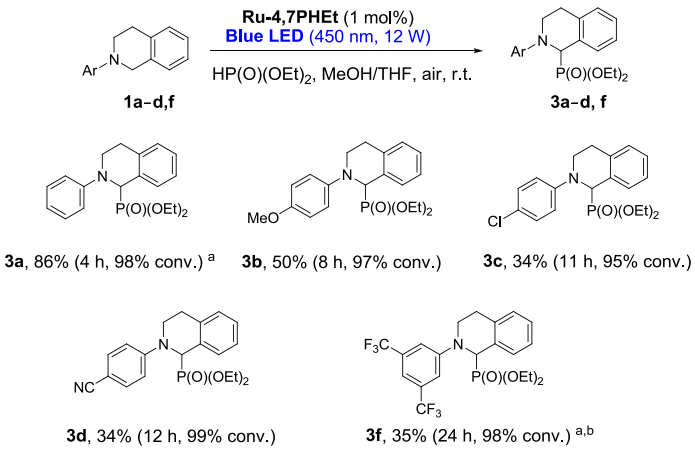

Scheme 4. Phosphonylation of *N*-aryl-1,2,3,4-tetrahydroisoquinolines. Reaction conditions: **1** (0.375 mmol), **Ru-4,7PHEt** (1 mol%), $HP(O)(OEt)_2$ (62 μL, 0.488 mmol, 1.3 equiv.), THF/MeOH (1:1 v/v, 1.5 mL), air, blue LED (12 W), r.t.. The yields and conversions were determined by ^{1}H NMR spectroscopy of reaction mixtures. 1,3-Dimethoxybenzene was used as an internal standard (Figures S35 and S36). [a] MeOH (1.5 mL), was used as a solvent. [b] Isolated yield after column chromatography. 2-(3',5'-Bis(trifluoromethyl)phenyl-3,4-dihydroisoquinolin-1(2H)-one (10%) was isolated as a side product.

Thus, whatever the solvent employed, all phosphonates were obtained in only moderate yields (34–50%), regardless of the nature of the substituent on the phenyl residue. The negative influence of THIQ substitution in this reaction is not yet fully understood but our data correlate nicely with the results obtained when exploring electrochemical coupling of THIQs and diethyl *H*-phosphonate.[69] It is also worthy to note that no better homogeneous Ru(II) photocatalysts have been reported for this reaction, to the best of our knowledge. A significant improvement in the phosphonylation of functionalized THIQs was achieved only when a MOF containing photoactive 1,4,5,8-naphthalenediimide residues in the linkers was doped with $[Ru(bpy)_3]^{2+}$ catalytic centers.[70] This exceptional efficiency is likely to be explained by the participation of the solid support in the photocatalytic transformation.

The iminium ions also serve as valuable intermediates in synthesis of α-aminonitriles (Strecker reaction) which are essential building blocks for the preparation of α-amino acids and various heterocyclic compounds including imidazoles and alkaloids. By utilizing a homogeneous photoredox catalyst and visible light irradiation, the aerobic oxidative cyanation of tertiary amines becomes feasible under mild conditions.[71] This method allows for the functionalization of both cyclic and linear tertiary amines. We have shown that **Ru-4,7PHEt**, when used in methanol, can replace

reported Ir(III) photocatalysts and afford the target products 6 and 7 in good yields for both THIQ **1a** and *N*,*N*-dimethylaniline **5** (Scheme 5). As in aza-Henri reaction, the product yields were lower (10–20%) compared to those reported for Ir(III) photocatalysts.[71] Nevertheless, this method may be a useful alternative due to its cost-efficiency.

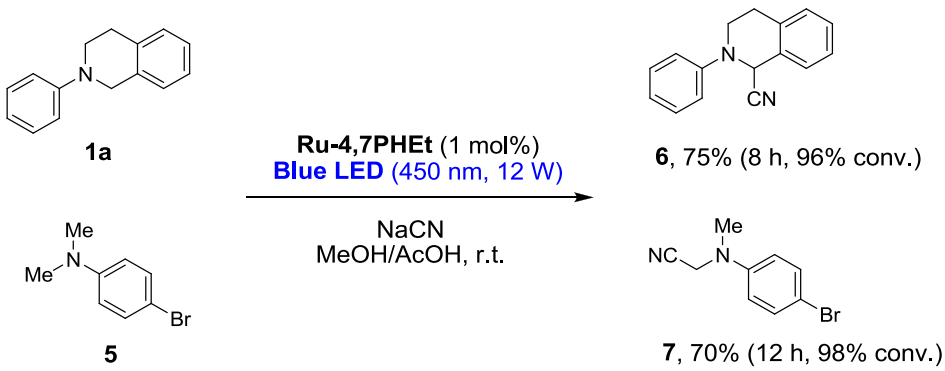

Scheme 5. Visible light photoredox-catalyzed oxidative cyanation of tertiary amines. Reaction conditions: **1a** or **5** (0.5 mmol), NaCN (40 mg, 0.75 mmol, 1.5 equiv.), **Ru-4,7PHEt** (1 mol%), MeOH (3 mL), AcOH (1 mL), air, blue LED (12 W), r.t. The yields and conversions were determined by NMR ^{1}H analysis of reaction mixtures. 1,3-Dimethoxybenzene was used as internal standard.

Showing the efficiency of **Ru-Pcat-A** in the visible light photoredox-catalyzed *α*-functionalization of tertiary amines by nitromethane, diethyl *H*-phosphonate and cyanides, we explored the catalyst recycling and reuse in the nitromethylation and phosphonylation of **1a** using the most active complex **Ru-4,7PHEt** (Figures 6 and S33–S37, Tables S9 and S11). After reaction completing, the catalyst was extracted into an aqueous phase, which was subsequently evaporated under reduced pressure to dryness. The residue thus obtained was dissolved in MeOH and introduced into the next catalytic cycle.

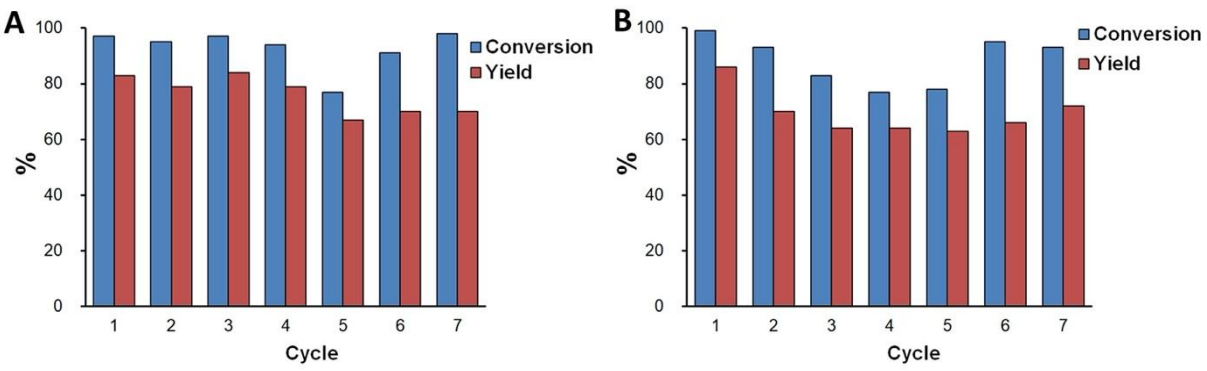

Figure 6. (A) Recycling **Ru-4,7PHEt** in the nitromethylation of THIQ **1a**. The irradiation time was 10 h for 1st to 5th cycles, 14 h for 6th cycle and 27 h for 7th cycle. (B) Recycling **Ru-4,7PHEt** in the phosphonylation of THIQ **1a**. The irradiation time was 4 h for 1st to 5th cycles, 6 h for 6th cycle and 14 h for 7th cycle.

In Figures 6A and S37A and Table S9, we present the results of the nitromethylation reaction. Five consecutive cycles of the reaction were performed, each irradiated for 10 h using blue LED light. The conversion remained high for the first four cycles, with only a 20% decrease observed in the fifth cycle. By increasing the reaction time to 14 h and 27 h, we were able to perform the transformation of starting **1a** in the 6^{th} and 7^{th} cycles, respectively, achieving almost complete conversion.

We also investigated the recycling of **Ru-bpy** using the same post-synthetic treatment. The recycled **Ru-bpy** complex exhibited significantly lower efficiency already in the 2^{nd} cycle, requiring a four fold increase in reaction time to achieve complete conversion of the starting amine (Table S10).

The reaction of **1a** with diethyl *H*-phosphonate was stopped after 4 h of irradiation in each of the five consecutive cycles (Figures 6B and S37B and Table S12). As shown in Figure 6B, a conversion of over 77% was achieved in all these experiments, and the reaction selectivity slightly decrease only after the 1^{st} cycle. However, in the subsequent two catalytic cycles (6^{th} and 7^{th} cycles), we had to increase the irradiation time to 6 h and 14 h, respectively, to achieve a similar conversion and product yield.

Thus, our comparative studies of the photocatalytic properties of four Ru(II) complexes from the **Ru-Pcat-A** series have shown that the **Ru-4,7PHEt** complex, bearing lateral monoethyl phosphonate residues, exhibits excellent photocatalytic properties in visible light photoredox-catalyzed α-functionalization of tertiary amines. Additionally, this complex can be recycled by extracting in aqueous phase and reused. This enable a substantial increase in the Turn-Over Number (TON) of the photoredox catalyst while maintaining a high overall Turn-Over Frequency (TOF) and preserving reaction selectivity (Table S13).

CONCLUSIONS

In this study, we have demonstrated that Ru(II) complexes with negatively charged phenanthroline ligands show promise as recyclable homogeneous photoredox catalysts, providing a cost-efficient alternative to heterogenized Ru(II) complexes.

Specifically, we explored $[Ru(phen)(bpy)_2]^{2+}$-type complexes incorporating phosphonate-substituted phen ligands (**Ru-Pcat-A**) which exist as uncharged species in aqueous solutions across a wide pH range (> 2.5).

A practical synthetic approach was developed to prepare symmetrically disubstituted (4,7- and 3,8-substituted) Ru(II) complexes with lateral phosphonic acid groups (**Ru-4,7PH** and **Ru-3,8PH**) and their monoalkyl esters (**Ru-4,7PHEt** and **Ru-3,8PHEt**) in excellent yields (87–99%) without the need for expensive reagents and size exclusion chromatography. The complexes were synthesized in a two-step procedure starting from commercially available *cis*-$[Ru(bpy)_2Cl_2]$ and suitable phen ligands with diethoxyphosphoryl substituents. The resulting complexes were hydrolyzed in water without adding acids or bases. By varying the temperature during this step, both phosphonic acid-substituted derivatives **Ru-4,7PH** and **Ru-3,8PH** and analogous complexes with alkyl phosphonate groups **Ru-4,7PHEt** and **Ru-3,8PHEt** were obtained selectively and isolated in high yields.

The coordination mode of ditopic phen ligands and kinetic inertness of the newly synthesized complexes were confirmed through single crystal X-ray analysis of **Ru-4,7PH** and NMR studies of other complexes **Ru-Pcat-A**. After confirming that the complexes exhibit good solubility and high photostability in both aqueous media and polar protic and aprotic organic solvents (DMF and DMSO), we systematically investigated their optical properties. We found that the light absorption by **Ru-Pcat-A** was quite similar, regardless of the nature of substituents on the phosphonate group or the location of these groups on the phen core. However, the emission observed in Ar-saturated aqueous solutions of these complexes was noticeably influenced by the substitution pattern of the heterocycle and quantum yields reached approximately 0.11 for **Ru-4,7PHEt** and **Ru-4,7PH**, both of which bear the phosphonate substituent at positions 4 and 7 of the heterocycle. This value is twice as high as that of the classical $[Ru(bpy)_3]^{2+}$ photoredox catalyst in Ar-saturated aqueous solutions.

The photocatalytic performance of **Ru-Pcat-A** was investigated using visible light photoredox catalytic nitromethylation, phosphonylation and cyanation of tertiary amines. In the majority of the studied reactions, the complex **Ru-4,7PHEt** exhibited higher efficiency compared to the benchmark photocatalyst **Ru-bpy**, and it could be readily separated from the products using extraction in water. Seven consecutive catalytic cycles of nitromethylation and phosphonylation of *N*-phenyl-substituted THIQ was successfully performed using this homogeneous photoredox catalyst.

Thus, our research advances the development of efficient and sustainable homogeneous PCs which are crucial for the industrial application of visible light photoredox catalyzed reactions.

EXPERIMENTAL

Materials and methods

Unless otherwise noted, all chemicals and starting materials were obtained commercially from Acros and Aldrich–Sigma Co and used without further purification. Phosphonate-substituted 1,10-phenanthrolines **3,8PEt** and **4,7PEt** were obtained by using previously reported procedures.[72] *Cis*-[$Ru(bpy)_2Cl_2$] was prepared from $RuCl_3 \times H_2O$ as reported previously.[73] *N*-Aryl-tetrahydroisoquinolinones **1a-f** were prepered from 1,2,3,4-tetrahydroisoquinolinone *via* Buchwald-Hartwig reaction as reported in the litterature.[69,74,75] Preparative column chromatography was carried out using Silica gel 60 (40–63 μm) from Merck Co. Toluene was distilled over sodium; EtOH was distilled over CaO; MeOH was used freshly distilled. Synthesis of Ru(II) complexes **Ru-3,8PEt** and **Ru-4,7PEt** was conducted in Monowave 300 Microwave reactor (Anton Paar Co) as reported previously.[27] The reactions were performed in Glass tubes provided by Anton Paar Co (G30 and G10 models). ^{1}H, $^{13}C\{^{1}H\}$, $^{31}P\{^{1}H\}$ and $^{19}F\{^{1}H\}$ NMR spectra were recorded with Bruker Avance-400 spectrometer in $CDCl_3$, D_2O or CD_3CN using the residual signals of solvents as internal standards. 2D NMR spectra of **Ru-4,7PH**, **Ru-4,7PEt** and **Ru-phen** were recorded on the Agilent 400-MR spectrometer. MALDI TOF mass-spectra were obtained with Bruker Daltonics Autoflex II mass spectrometer in positive ion mode with dithranol matrix and polyethylene glycols (PEG-600 + PEG-1000) as internal standards. Accurate mass measurements (HRMS) were made on a THERMO LTQ Orbitrap XL equipped with an electrospray ionisation (ESI) source in positive mode. Solutions in $CHCl_3$/methanol (1:1) were used for the analysis and the spectra were recorded at the "Centre Commun de Spectrométrie de Masse" (UCBL, Villeurbanne, France). FTIR spectra were registered on Nicolet iS 5 and Bruker Vector 22 spectrophotometers. Micro-ATR accessory (Pike) was used in order to obtain FTIR spectra of polycrystalline solid complexes. UV–vis spectra were registered with a Hitachi U-2900 device (Tokyo, Japan) in a quartz cuvette (Hellma, l = 1 cm). Fluorescence spectra were registered

with Horiba Jobin Yvon Fluoromax-2 apparatus (Edison, NJ, USA) in a quartz cuvette (Hellma, l = 1 cm), (shutter: Auto Open, excitation slit = 3 nm and emission slit = 3 nm). All fluorescence spectra were corrected.

Fluorescence quantum yields were measured in Ar-saturated deionized water at 293 K by a relative method using $[Ru(bpy)_3](PF_6)_2$ (Φ_F = 9.4% in acetonitrile) as a standard.[76] The following equation was used to determine the relative fluorescence quantum yield:

$$\Phi_x = \Phi_{st} \times ((F_x \times A_{st} \times \eta_x^2)/(F_{st} \times A_x \times \eta_{st}^2))$$

where A is the absorbance (in the range of 0.01–0.1 A.U.), F is the area under the emission curve, η is the refractive index of the solvents (at 293 K) used in measurements, and the subscripts s and x represent standard and studied compound, respectively. The following refractive index value is used: 1.3460 for CH_3CN and 1.3325 for water. At least 4 points were used for each sample.

Synthesis of ruthenium complexes

Complexes Ru-3,8PHEt and Ru-4,7PHEt. ***General procedure.*** Complex *cis*-$[Ru(bpy)_2Cl_2]$ (0.207 mmol, 100 mg) was charged into a G30 glass tube equipped with a stir bar. The phen ligand **3,8PEt** or **4,7PEt**, (0.221 mmol, 1.07 equiv., 100 mg) was dissolved in EtOH (4 mL) and added into the reaction vessel. The tube was sealed and heated in MW reactor at 100 °C for 1 h. The reaction mixture was evaporated under reduced pressure and the residue was dissolved in water (5 mL). This solution was washed with CH_2Cl_2 until the organic phase became uncolored and evaporated under reduced pressure. The residue (crude **Ru-3,8PEt** or **Ru-4,7PEt**) was analyzed by ^1H NMR spectroscopy and introduced in the next step without additional purification.

This solid residue and 15 mL of water were placed in a glass pressure resistant tube with a screw cap (Synthware®) equipped with a stir bar. The vessel was sealed and put into preheated oil bath. The reaction mixture was stirred at 130 °C for 4 h. After cooling to room temperature, the precipitate was filtered through 200 nm syringe filter (Chromafil®), and the filter was washed with water (10 mL). The filtrates were combined and evaporated under reduced pressure giving the product as glassy red solid.

[Ru(3,8-P(O)(OH)(OEt)-Phen)(bpy)$_2$]Cl$_2$×4.5H$_2$O (**Ru-3,8PHEt**) was obtained from **3,8PEt** (100 mg, 0.221 mmol) and *cis*-[Ru(bpy)$_2$Cl$_2$] (100 mg, 0.207 mmol). Yield: 184 mg (92%), deep reddish glassy solid. ^{1}H NMR (D$_2$O, 400 MHz): δ 8.89(d, 2H, $J_{H,P}$ = 12.8 Hz, H4 and H7 (Phen)), 8.48–8.46 (m, 2H, H3 (bpy)), 8.43–8.40 (m, 2H, H3 (bpy)), 8.18 (s, 2H, H5 and H6 (Phen)), 8.12 (d, 2H, $^3J_{H,P}$ = 6.5 Hz, H2 and H9 (Phen)), 7.99–7.95 (m, 2H, H4 (bpy)), 7.87–7.83 (m, 4H, H4 (bpy) and H6 (bpy)), 7.51–7.50 (m, 2H, H6 (bpy)), 7.33–7.30 (m, 2H, H5 (bpy)), 7.07–7.05 (m, 2H, H5 (bpy)), 3.60–3.48 (m, 4H, CH$_2$O), 0.81 (t, $^3J_{H,H}$ = 7.0 Hz, 6H, CH$_3$). ^{31}P{^{1}H} NMR (D$_2$O, 162 MHz): δ 8.0 (s, 2P, P(O)(OH)(OEt)). IR (neat): 3342 (m, OH), 3264 (m), 3104 (w), 3072 (w), 2973 (w), 2932 (w), 2897 (w), 2819 (w), 1646 (m, HOH), 1601 (m), 1464 (m), 1443 (m), 1420 (m), 1387 (w), 1366 (w), 1341 (w), 1312 (w), 1219 (s, P=O), 1137 (m, P–OC), 1099 (w) 1069 (s, P–OC), 1031 (s, P–OC), 939 (s, P–OC), 801 (m), 764 (m, P–C), 730 (m), 724 (m), 707 (m) cm^{-1}. *Anal*. Calcd. for C$_{36}$H$_{43}$Cl$_2$N$_6$O$_{10.5}$P$_2$Ru: C, 44.9; H, 4.51; N, 8.74; 961.69; Found: C, 44.93; H, 3.79; N, 8.63. HRMS (ESI) m/z: [M^{2+}–H$^+$]$^+$ Calcd. for C$_{36}$H$_{33}$N$_6$O$_6$P$_2$Ru$^+$ 809.0975; Found 809.0985.

[Ru(4,7-P(O)(OH)(OEt)-Phen)(bpy)$_2$]Cl$_2$×H$_2$O (**Ru-4,7PHEt**) was obtained from **4,7PEt** (100 mg, 0.221 mmol) and *cis*-[Ru(bpy)$_2$Cl$_2$] (100 mg, 0.207 mmol). Yield: 183 mg (99%), deep reddish glassy solid. ^{1}H NMR (D$_2$O, 400 MHz): δ 8.73 (s, 2H, H5 and H6 (Phen)), 8.46–8.44 (m, 2H, H3 (bpy)), 8.42–8.40 (m, 2H, H3 (bpy)), 8.18 (dd, 2H, $^4J_{H,P}$ = 2.8 Hz, $^3J_{H,H}$ = 5.3 Hz, H2 and H9 (Phen)), 8.00–7.96 (m, 2H, H4 (bpy)), 7.86 (dd, 2H, $^3J_{H,P}$ = 13.4 Hz, $^3J_{H,H}$ = 5.3 Hz, H3 and H8 (Phen)), 7.88–7.84 (m, 2H, H4 (bpy)), 7.80–7.79 (m, 2H, H6 (bpy)), 7.43–7.42 (m, 2H, H6 (bpy)), 7.32–7.29 (m, 2H, H5 (bpy)), 7.09–7.06 (m, 2H, H5 (bpy)) , 3.84–3.77 (m, 4H, CH$_2$O), 1.04 (t, $^3J_{H,H}$ = 7.0 Hz, 6H, CH$_3$). ^{31}P{^{1}H} NMR (D$_2$O, 162 MHz): δ 7.7 (s, 2P, P(O)(OH)(OEt)). IR (neat): 3377 (m, OH), 3106 (w), 3070 (m), 2977 (w), 2930 (w), 2902 (w), 1646 (w, HOH), 1602 (w), 1464 (m), 1444 (m), 1419 (w), 1312 (w) 1269 (w), 1228 (m, P=O), 1159 (m, P=O), 1096 (w), 1068 (w), 1036 (s, P–OC), 948 (m, P–OH), 850 (m), 805 (w), 768 (m, P–C), 730 (w), 682 (w), 668 (w), 611 (w) cm^{-1}. Anal. Calcd. for C$_{36}$H$_{36}$Cl$_2$N$_6$O$_7$P$_2$Ru: C, 48.12; H, 4.04; N, 9.35; 898.00. Found: C, 47.68; H, 3.80; N, 9.38. HRMS (ESI) m/z: [M^{2+}–H$^+$]$^+$ Calcd. for C$_{36}$H$_{33}$N$_6$O$_6$P$_2$Ru$^+$ 809.0975; Found 809.0985.

Complexes Ru-3,8PH and Ru-4,7PH. ***General procedure***. Complex *cis*-[$Ru(bpy)_2Cl_2$] (0.207 mmol, 100 mg) was charged into a G30 glass tube equipped with a stir bar. The phen ligand **3,8PEt** or **4,7PEt** (0.221 mmol, 1.07 equiv., 100 mg) was dissolved in EtOH (4 mL) and added into the reaction vessel. The tube was sealed and heated in MW reactor at 100 °C for 1 h. The reaction mixture was evaporated under reduced pressure and the residue was dissolved in water (5 mL). This solution was washed with CH_2Cl_2 until the organic phase became uncolored and evaporated under reduced pressure. The residue (crude **Ru-3,8PEt** or **Ru-4,7PEt**) was analyzed by ^{1}H NMR spectroscopy and introduced in the next step without additional purification.

This solid residue and 15 mL of water were placed in a in a glass pressure resistant tube with a screw cap (Synthware ®) equipped with a stir bar. The vessel was sealed and put into preheated oil bath. The reaction mixture was stirred at 150 °C for 48 h. After cooling to room temperature, the precipitate was filtered through 200 nm syringe filter (Chromafil®), and the filter was washed with water (10 mL). The aqueous filtrates were combined and evaporated under reduced pressure giving the product as glassy red solid.

[Ru(3,8-P(O)(OH)$_2$-Phen)(bpy)$_2$]Cl$_2$×2H$_2$O (**Ru-3,8PH**) was obtained from **3,8PEt** (100 mg, 0.221 mmol) and *cis*-[$Ru(bpy)_2Cl_2$] (100 mg, 0.207 mmol). Yield: 155 mg (87%), deep red glassy solid. ^{1}H NMR (D_2O, 400 MHz): δ 8.68 (d, 2H, $^3J_{H,P}$ = 13.0 Hz, H4 and H7 (Phen)), 8.42–8.40 (m, 2H, H3 (bpy)), 8.37–8.35 (m, 2H, H3 (bpy)), 8.20 (d, 2H, $^3J_{H,P}$ = 6.2 Hz, H2 and H9 (Phen)), 8.13 (s, 2H, H5 and H6 (Phen)), 7.94–7.90 (m, 2H, H4 (bpy)), 7.83–7.79 (m, 2H, H4 (bpy)), 7.79–7.78 (m, 2H, H6 (bpy)), 7.47–7.46 (m, 2H, H6 (bpy)), 7.28–7.25 (m, 2H, H5 (bpy)), 7.04–7.01 (m, 2H, H5 (bpy)). ^{31}P{^{1}H} NMR (D_2O, 162 MHz): δ 6.2 (s, 2P, P(O)$(OH)_2$). IR (neat): 3354 (s, OH), 3107 (w, P–OH), 3071 (w), 2974 (w), 2922 (w), 2824 (m), 1844 (m), 1635 (m, HOH), 1602 (m), 1464 (m), 1444 (m), 1422 (m), 1369 (w), 1311 (w), 1213 (m, P=O), 1140 (m, P=O), 1068 (w), 1022 (m), 963 (s, P–O), 912 (s, P–OH), 765 (s, P–C), 723 (m), 709 (m) cm^{-1}. *Anal*. Calcd. for $C_{32}H_{30}Cl_2N_6O_8P_2Ru$: C, 44.66; H, 3.51; N, 9.77; 916.06; Found: C, 44.99; H, 3.25; N, 9.35. HRMS (ESI) m/z: $[M^{2+}–2H^++Na]^+$ Calcd. for $C_{32}H_{24}N_6NaO_6P_2Ru^+$ 775.0168; Found 775.0171.

[Ru(4,7-P(O)(OH)$_2$-Phen)(bpy)$_2$]Cl$_2$×2H$_2$O (**Ru-4,7PH**) was obtained from **4,7PEt** (100 mg, 0.221 mmol) and *cis*-[$Ru(bpy)_2Cl_2$] (100 mg, 0.207 mmol). Yield: 167 mg

(94%), deep reddish glassy solid. ^{1}H NMR (D_2O, 400 MHz): δ 8.84 (s, 2H, H5 and H6 (Phen)), 8.53–8.51 (m, 2H, H3 (bpy)), 8.48–8.46 (m, 2H, H3" (bpy)), 8.18 (dd, 2H, $^{4}J_{H,P}$ = 2.8 Hz, $^{3}J_{H,H}$ = 5.3 Hz, H2 and H9 (Phen)), 8.06–8.02 (m, 2H, H4 (bpy)), 7.96 (dd, 2H, $^{3}J_{H,P}$ = 13.5 Hz, $^{3}J_{H,H}$ = 5.3 Hz, H3 and H8 (Phen)), 7.94–7.89 (m, 2H, H4" (bpy)), 7.87–7.85 (m, 2H, H6 (bpy)), 7.51–7.50 (m, 2H, H6" (bpy)), 7.39–7.36 (m, 2H, H5 (bpy)), 7.14–7.11 (m, 2H, H5" (bpy)). ^{13}C{^{1}H} NMR (D_2O, 125 MHz): δ 157.0 (s, 2C, C2 (bpy)), 156.9 (s, 2C, C2" (bpy)), 152.0 (d, 2C, $^{3}J_{C,P}$ = 12.8 Hz, C2 and C9), 151.5 (s, 2C, C6 (bpy)), 151.3 (s, 2C, C6" (bpy)), 148.0 (dd, 2C, $^{3}J_{C,P}$ = 10.5 Hz, $^{4}J_{C,P}$ = 2.3 Hz, C1 and C10), 142.3 (d, 2C, $^{1}J_{C,P}$ = 168.8 Hz, C4 and C7), 137.8 (s, 2C, C4 (bpy)), 137.7 (s, 2C, C4"(bpy)), 130.1 (d, 2C, $^{3}J_{C,P}$ = 9.4 Hz, C1a and C10a), 127.8 (d, 2C, $^{3}J_{C,P}$ = 7.9 Hz, C3 and C8), 127.6 (d, 2C, $^{3}J_{C,P}$ = 4.5 Hz, C5 and C6 (Phen)), 127.2 (s, 2C, C5 (bpy)), 127.0 (s, 2C, C5" (bpy)), 124.04 (s, 2C, C3 (bpy)), 124.01 (s, 2C, C3" (bpy)). ^{31}P{^{1}H} NMR (D_2O, 162.5 MHz): δ 5.4 (s, 2P, $P(O)(OH)_2$). IR (neat): 3301 (s), 3107 (w), 3070 (w), 2932 (w), 2911 (w), 2821 (w), 1623 (w, HOH), 1601 (m), 1490 (w), 1464 (m), 1443 (s), 1419 (m), 1311 (w), 1269 (w), 1219 (m, P=O), 1190 (m), 1158 (m, P=O), 1122 (w), 1094 (w), 1067 (w), 1022 (s, P–O), 924 (s, P–O), 908 (s, P–OH), 843 (m), 825 (w), 798 (w), 761 (s, P–C), 728 (m) cm^{-1}. Anal. Calcd. for $C_{32}H_{30}Cl_2N_6O_8P_2Ru$: C, 44.66; H, 3.51; N, 9.77; 916.06; Found: C, 44.84; H, 3.11; N, 9.31. HRMS (ESI) m/z: $[M^{2+}–H^{+}]^{+}$ Calcd. for $C_{32}H_{25}N_6O_6P_2Ru^{+}$ 753.0349; Found 753.0357.

Single crystal X-ray analysis of Ru-4,7PH

Red plate-shaped crystals of **Ru-4,7PH** suitable for single-crystal X-ray diffraction were crystallized by slow evaporation of methanol solution through the silicon septum during *ca.* 30 days. For single crystal of **Ru-4,7PH** 51030 reflection with 2θ max = 58° were measured on a Bruker D8 QUEST single-crystal X-ray diffractometer equipped with PHOTONII detector, charge-integrating pixel array detector (CPAD), laterally graded multilayer (Goebel) mirror and microfocus Mo-target X-ray tube (λ = 0.73071 Å). Data reduction and integration were performed with the Bruker software package SAINT. **Ru-4,7PH** at 110 K, monoclinic; space group *P21/n*; cell parameters: a = 14.6262(19), b = 14.7930(18), c = 17.000(2) (7) Å, β = 104.493(4)°, V = 3561.2(8)Å^3 , Z = 4. Crystal structure solution and refinement were performed using SHELX-2018 package.[77] Atomic positions were located using

dual method and refined using a combination of Fourier synthesis and least-square refinement in isotropic and anisotropic approximations. The analysis of the Fourier density synthesis has revealed that part of phenanthroline one of the PO_3 group is disordered by two positions with equal occupancies. The refinement was performed with EADP instruction for disordered by two positions of PO_3 and phenanthroline group. All hydrogen atoms (with the exception of PO_3H, oxonium and water molecules) were placed in the calculated positions and allowed to ride on their parent atoms. Refinement was made against 9473 reflections. 522 parameters were refined using 0 restraints. The final R = 0.0600 against 6766 observed reflection, GOF = 1.009, wR^2 = 0.1627 for all reflections. The structure has been deposited at the Cambridge Crystallographic Data Center with the reference CCDC number 2291633. These data can be obtained free of charge from the CCDC *via* http://www.ccdc.cam.ac.uk/data_request/cif.

Oxidative nitromethylation of *N*-Aryl-1,2,3,4-tetrahydroisoquinolines (THIQs). ***General procedure*.** THIQ (0.3 mmol) and Ru(II) complex (1 mol%) were placed into 15 mL polypropylene centrifuge tube equipped with a stir bar. Nitromethane (1.2 mL) and methanol (0.8 mL) were added, the tube was closed by a septum equipped with a glass outlet attached to a silicone tube (Figure S32) and the reaction mixture was stirred at room temperature under irradiation by blue LED (Figure S32). The reaction was periodically monitored by ^{1}H NMR spectroscopy of aliquots (30 μL) taken from the reaction mixture. When the reaction was complete, the reaction mixture was diluted with CH_2Cl_2 (10 mL), washed with water (2 × 5 mL), and 1,3-dimethoxybenzene (1 equiv.) was added to the organic phase. Then, the organic phase was evaporated under reduced pressure and analyzed by ^{1}H NMR spectroscopy. All compounds thus prepared (**2a–e**) were reported previously, and their spectral data were consistent with those reported in the literature. ^{1}H NMR yields are provided below.

1-(Nitromethyl)-2-phenyl-1,2,3,4-tetrahydroisoquinoline (2a).[74] Yield: 85%. ^{1}H NMR ($CDCl_3$, 400 MHz): δ 7.39–7.12 (m, 5H), 7.03 (d, 2H, *J* = 7.7 Hz), 6.89 (t, 1H, *J* = 7.3 Hz), 5.59 (t, 1H, *J* = 7.3 Hz), 4.91–4.86 (m, 1H), 4.61–4.56 (m, 1H), 3.69–3.60 (m, 2H), 3.18–3.06 (m, 1H), 2.86–2.74 (m, 1H).

1-(Nitromethyl)-2-(4-methoxyphenyl)-1,2,3,4-tetrahydroisoquinoline (2b).[74] Yield: 70%. ^{1}H NMR ($CDCl_3$, 400 MHz): *δ* 7.16–7.10 (m, 4H), 6.87 (d, 2H, *J* = 9.1 Hz), 6.76

(d, 2H, *J* = 9.1 Hz), 5.36–5.33 (m, 1H), 4.81–4.76 (m, 1H), 4.57–4.52 (m, 1H), 3.89 (s, 3H), 3.55–3.50 (m, 2H), 2.99–2.91 (m, 1H), 2.66–2.60 (m, 1H).

1-(Nitromethyl)-2-(4-chlorophenyl)-1,2,3,4-tetrahydroisoquinoline (2c).[79] Yield: 73%. ^{1}H NMR ($CDCl_3$, 400 MHz): δ 7.27–7.21 (m, 6H), 6.92 (d, 2H, *J* = 9.1 Hz), 5.53–5.50 (m, 1H), 4.87–4.82 (m, 1H), 4.60–4.55 (m, 1H), 3.66–3.59 (m, 2H), 3.11–2.99 (m, 1H), 2.81–2.75 (m, 1H).

1-(Nitromethyl)-2-(4-cyanophenyl)-1,2,3,4-tetrahydroisoquinoline (2d).[74] Yield: 40%. ^{1}H NMR ($CDCl_3$, 400 MHz): δ 7.50 (d, 2H, *J* = 9.0 Hz), 7.22–7.15 (m, 4H), 6.96 (d, 2H, *J* = 9.0 Hz), 5.52 (t, 1H, *J* = 7.2 Hz), 4.86–4.81 (m, 1H), 4.62–4.57 (m, 1H), 3.86 (t, 2H, *J* = 6.2 Hz), 3.13–3.05 (m, 1H), 2.91–2.86 (m, 1H).

1-(Nitromethyl)-2-(4-bromophenyl)-1,2,3,4-tetrahydroisoquinoline (2e).[74] Yield: 75%. ^{1}H NMR ($CDCl_3$, 400 MHz): δ 7.31(d, 2H, *J* = 9.1 Hz), 7.25–7.17 (m, 4H), 6.82 (d, 2H, *J* = 9.1 Hz), 5.46–5.44 (m, 1H), 4.85–4.80 (m, 1H), 4.58–4.53 (m, 1H), 3.61–3.55 (m, 2H), 3.07–2.97 (m, 1H), 2.79–2.72 (m, 1H).

Photocatalyst recycling. Upon reaction completion, CH_2Cl_2 (4 mL) was added to the reaction mixture. The mixture was then extracted with water until an uncolored aqueous phase was obtained (2 × 3 mL). The combined aqueous phases were evaporated under reduced pressure. To introduce the recovered photocatalyst into the next catalytic cycle, the residue was dissolved in MeOH (1 mL).

Oxidative phosphonylation of *N*-Aryl-1,2,3,4-tetrahydroisoquinolines (THIQs). *General procedure.* THIQ (0.375 mmol) and Ru(II) complex (1 mol%) were placed into 15 mL polypropylene centrifuge tube equipped with a stir bar. Solvent (MeOH or MeOH/THF (1:1 v/v), 1.5 mL) and diethyl *H*-phosphonate (62 μL, 0.476 mmol, 1.27 equiv.) were added, and the tube was closed by the septum equipped with a glass outlet attached to a silicone tube (Figure S32) and the reaction mixture was stirred at room temperature under irradiation by a blue LED (Figure S32). The reaction was periodically monitored by ^{1}H NMR spectroscopy of aliquots (30 μL) taken from the reaction mixture. When the reaction was complete, the reaction mixture was diluted with CH_2Cl_2 (10 mL), washed with water (2 × 5 mL), and 1,3-dimethoxybenzene (1 equiv.) was added to the organic phase. Then, the organic phase was evaporated under reduced pressure and analyzed by ^{1}H NMR spectroscopy. All compounds thus prepared (**3a**–**d**) were

reported previously, and their spectral data were consistent with those reported in the literature. ^{1}H NMR yields are provided below.

Diethyl (2-phenyl-1,2,3,4-tetrahydroisoquinolin-1-yl)phosphonate (**3a**).[69] The reaction was performed in MeOH (1.5 mL). Yield: 76%. ^{1}H NMR ($CDCl_3$, 400 MHz): δ 7.40 (br d, 1H, J_{obs} = 6.4 Hz), 7.29–7.15 (m, 5H), 7.03 (d, 2H, J = 8.3 Hz), 6.81 (t, 1H, J = 7.2 Hz), 5.22 (d, 1H, $J_{H,P}$ = 20.0 Hz, P-C-H), 4.19–3.89 (m, 5H), 3.67–3.61 (m, 1H), 3.12–2.97 (m, 2H), 1.26 (t, 3H, J = 7.1 Hz), 1.16 (t, 3H, J = 7.1 Hz).

Diethyl (2-(4-methoxyphenyl)-1,2,3,4-tetrahydroisoquinolin-1-yl)phosphonate (**3b**).[69] The reaction was performed in THF/MeOH solvent mixture (1 : 1 v/v, 1.5 mL). Yield: 35%. ^{1}H NMR ($CDCl_3$, 400 MHz): δ 7.36 (m, 1H), 7.24–7.12 (m, 3H), 6.91 (d, 2H, J = 9.0 Hz), 6.80 (d, 2H, J = 9.0 Hz), 5.04 (d, 1H, $J_{H,P}$ = 21.5 Hz, P-C-H), 4.11–3.91 (m, 5H), 3.57–3.49 (m, 1H), 2.98–2.93 (m, 2H), 1.25 (t, 3H, J = 7.0 Hz), 1.16 (t, 3H, J = 7.0 Hz).

Diethyl (2-(4-chlorophenyl)-1,2,3,4-tetrahydroisoquinolin-1-yl)phosphonate (**3c**).[69] The reaction was performed in THF/MeOH (1 : 1 v/v, 1.5 mL). Yield: 35%. ^{1}H NMR ($CDCl_3$, 400 MHz): δ 7.36 (br d, 1H, J = 6.4 Hz), 7.24–7.12 (m, 5H), 6.99 (d, 2H, J = 9.0 Hz), 5.12 (d, 1H, $J_{H,P}$ = 19.2 Hz, P-C-H), 4.13–3.85 (m, 5H), 3.53–3.48 (m, 1H), 3.12–2.94 (m, 2H), 1.23 (t, 3H, J = 7.0 Hz), 1.14 (t, 3H, J = 7.0 Hz).

Diethyl (2-(4-cyanophenyl)-1,2,3,4-tetrahydroisoquinolin-1-yl)phosphonate (**3d**).[69] The reaction was performed in THF/MeOH (1 : 1 v/v, 1.5 mL). Yield: 34%. ^{1}H NMR ($CDCl_3$, 400 MHz): δ 7.53–7.43 (m, 2H), 7.34–7.27 (m, 1H), 7.20 (dd, J = 9.0, 3.6 Hz, 3H), 6.93 (d, J = 9.0 Hz, 2H), 5.19 (d, $J_{H,P}$ = 17.4 Hz, 1H), 4.18–3.70 (m, 5H), 3.64–3.46 (m, 1H), 3.42–3.20 (m, 1H), 2.98 (dd, J = 15.6, 9.0 Hz, 1H), 1.18 (t, 3H, J = 7.0 Hz), 1.08(t, 3H, J = 7.0 Hz).

Diethyl (2-(3,5-bis(trifluoromethyl)phenyl)-1,2,3,4-tetrahydroisoquinolin-1-yl)phosphonate (**3f**). The reaction was performed in MeOH (1.5 mL). Upon reaction completion, the reaction mixture was evaporated under reduced pressure. The product was isolated by column chromatography on silica gel eluting with pentane/ethyl acetate (gradient, 10:1 → 1:1). Yield: 63 mg (35%). ^{1}H NMR ($CDCl_3$, 400 MHz): δ 7.41–7.37 (m, 3H, Ar–$(CF_3)_2$), 7.30–7.22 (m, 4H, Ar–THIQ), 5.20 (d, 1H, $J_{H,P}$ = 16.9 Hz, PC-H), 4.16–3.81 (m, 5H, OCH_2 and N–C<u>H</u>–CH_2), 3.62–3.54 (m, 1H, N–C<u>H'</u>–CH_2), 3.51–3.41 (m, 1H, N–CH_2–C<u>H</u>), 3.09–3.00 (m, 1H, N– CH_2–C<u>H'</u>), 1.22 (t, 3H, J = 7.1 Hz, CH_3), 1.17 (t, 3H, J = 7.1 Hz, CH_3'). ^{13}C{^{1}H} NMR ($CDCl_3$, 125 MHz): δ 149.5 (d, $J_{C,P}$ = 2.3 Hz, 1C, C1 (Ph-$(CF_3)_2$)), 136.2 (d, 1C, $J_{C,P}$ = 5.2 Hz, C4' (THIQ)),

132.2 (q, 2C, $J_{C,F}$ = 32.6 Hz, $\underline{C}CF_3$), 130.0 (s, 1C, C1' (THIQ)), 128.4 (d, 1C, $J_{C,P}$ = 2.9 Hz, C6 (THIQ)), 128.3 (d, 1C, $J_{C,P}$ = 5.2 Hz, C5 (THIQ)), 128.2 (d, 1C, $J_{C,P}$ = 3.4 Hz, C8 (THIQ)), 123.7 (q, 2C, $J_{C,F}$ = 272.8 Hz, CF_3), 113.0 (m, 2C, C2 and C6 (Ph-$(CF_3)_2$)), 110.7–110.5 (m, 1C, C4 (Ph-$(CF_3)_2$)), 63.0 (d, 1C, $J_{C,P}$ = 7.6 Hz, OCH_2), 62.9 (d, 1C, $J_{C,P}$ = 7.7 Hz, OCH_2'), 58.6 (d, 1H, $J_{C,P}$ = 160.1 Hz, P-C-H), 43.9 (s, 1C, C3 (THIQ)), 27.5 (s, 1C, C4 (THIQ)), 16.2 (d, 1C, $J_{C,P}$ = 4.0 Hz, CH_3), 16.1 (d, 1C, $J_{C,P}$ = 4.1 Hz, CH_3'). $^{19}F\{^1H\}$ ($CDCl_3$, 162.5 MHz): δ -63.0 (s, 6F, CF_3). ^{31}P NMR ($CDCl_3$, 162.5 MHz): δ 21.34 (s, 1P, $P(O)(OEt)_2$). IR (neat): 1616 (m), 1477 (m), 1396 (m), 1349 (m), 1274 (m), 1247 (m, P=O), 1171 (m, P=O), 1126 (m), 1047 (m), 1022 (s, P–O), 967 (s, P–O), 846 (m), 783 (m) , 723 (s, P–C), 698 (w), 682 (w) cm^{-1}. HRMS (ESI) *m/z*: $[M+Na]^+$ Calcd. for $C_{21}H_{22}F_6NNaO_3P$ 504.1134; Found 504.1129.

2-(3,5-Bis(trifluoromethyl)phenyl)-3,4-dihydroisoquinolin-1(2H)-one.[80] Yield: 14 mg (10%). ^1H NMR ($CDCl_3$, 400 MHz): δ 7.41–7.37 (m, 3H), 8.18 (d, 1H, *J* = 7.7 Hz), 7.93 (s, 2H), 7.77 (s, 1H), 7.57–7.54 (m, 1H), 7.46–7.41 (m, 1H), 7.31 (d, 1H, *J* = 7.4 Hz), 4.10 (t, 2H, *J* = 6.4 Hz), 3.23 (t, 2H, $J_{H,H}$ = 6.4 Hz). $^{13}C\{^1H\}$ NMR ($CDCl_3$, 125 MHz): δ 164.3 (s, 1C, C=O), 144.3 (s), 138.2 (s), 132.8 (s), 131.9 (q, $J_{C,F}$ = 33.7 Hz, $\underline{C}CF_3$), 130.0 (s), 127.5 (s), 127.2 (s), 125.0 (br. m), 123.1 (q, $J_{C,F}$ = 272.8 Hz, CF_3), 119.5–119.3 (m), 49.0 (s), 28.4 (s).

Photocatalyst recycling. Upon reaction completion, CH_2Cl_2 (4 mL) was added to the reaction mixture. The mixture was then extracted with water until an uncolored aqueous phase was obtained (2 × 3 mL). The combined aqueous phases were evaporated under reduced pressure. To introduce the recovered photocatalyst into the next catalytic cycle, the residue was dissolved in MeOH (1 mL).

Oxidative cyanation of alkylarylamines. ***General procedure.*** Tertiary amine (0.5 mmol), NaCN (40 mg, 0.75 mmol, 1.5 equiv.) and Ru(II) complex (1 mol%) were placed into 15 mL polypropylene centrifuge tube equipped with stir bar. Acetic acid (1 mL) and MeOH (3 mL) were added, the tube was closed by the septum with glass outlet attached to a silicone tube (Figure S32) and the reaction mixture was stirred at room temperature under irradiation by blue LED. The reaction was periodically monitored by ^1H NMR spectroscopy of aliquot (30 μL) taken from the reaction mixture. When the reaction was complete, the reaction mixture was diluted with CH_2Cl_2 (10 mL), washed with water (2 × 5 mL), and 1,3-dimethoxybenzene (1 equiv.) was added to the organic phase. Then, the organic phase was evaporated under reduced

pressure and analyzed by ^{1}H NMR spectroscopy. Compound **4** and **6** thus prepared were reported previously, and their spectral data were consistent with those in the literature. ^{1}H NMR yields are provided below.

2-Phenyl-1,2,3,4-tetrahydroisoquinoline-1-carbonitrile (4).[81] Yield: 75%. ^{1}H NMR ($CDCl_3$, 400 MHz): δ 7.19 (m, 6H), 7.08 (m, 2H), 7.01 (m, 1H), 5.50 (s, 1H), 3.77 (m, 1H), 3.48 (m, 1H), 3.15, (m, 1H), 2.96 (m, 1 H).

2-((4-bromophenyl)(methyl)amino)acetonitrile (6).[82] Yield: 70%. ^{1}H NMR ($CDCl_3$, 400 MHz): δ 7.40 (d, 2H, *J* = 9.1 Hz), 6.74 (d, 2H, *J* = 9.1 Hz), 4.16 (s, 2H), 3.00 (s, 3H).

Author Contributions

Conceptualization, A.S.A. and A.B.L.; investigation, G.V.M. and A.S.A.; X-ray analysis, K.A.L.; NMR spectroscopy, V.A.R., A.B.L. and A.D.A.; supervision, I.P.B., funding acquisition, A.S.A. and I.P.B.; manuscript writing A.B.L. ; manuscript editing G.V.M., A.S.A. and A.B.L. All authors have read and agreed to the published version of the manuscript.

Conflicts of interest

There are no conflicts to declare.

Acknowledgements

We thank Dr. A. Cheprakov for fruitful and profitable discussions. This study was performed under financial support by the Russian Science Foundation, grants 19-13-00223P. K.A.L acknowledge financial support from the Ministry of Science and Higher Education of the Russian Federation within State Contract 075-15-2022-1117 from June 30, 2022 for crystal structure investigation. The Agilent 400-MR spectrometer and Bruker D8 Quest diffractometer purchased by the MSU Development Program.

REFERENCES

1.D. L. Ashford, M. K. Gish, A. K. Vannucci, M. K. Brennaman, J. L. Templeton, J. M. Papanikolas and T. J. Meyer, Molecular chromophore–catalyst assemblies for solar fuel applications, *Chem. Rev.*, 2015, **115**, 13006–13049.

2. Q. Zhao, F. Li and C. Huang, Phosphorescent chemosensors based on heavy-metal complexes, *Chem. Soc. Rev.*, 2010, **39**, 3007–3030.

3. F. Bella, C. Gerbaldi, C. Barolo and M. Grätzel, Aqueous dye-sensitized solar cells, *Chem. Soc. Rev.*, 2015, **44**, 3431–3473.

4. N. Hoffmann, Photochemical Reactions as key steps in organic synthesis, *Chem. Rev.*, 2008, **108**, 1052–1103.

5. A. A. Ghogare and A. Greer, Using singlet oxygen to synthesize natural products and drugs, *Chem. Rev.*, 2016, **116**, 9994–10034.

6. D. M. Schultz and T. P. Yoon, Solar synthesis: prospects in visible light photocatalysis, *Science*, 2014, **343**, 1239176.

7. J. M. R. Narayanam and C. R. J. Stephenson, Visible light photoredox catalysis: applications in organic synthesis, *Chem. Soc. Rev.*, 2011, **40**, 102–113.

8. C. K. Prier, D. A. Rankic and D. W. C. MacMillan, Visible Llght photoredox catalysis with transition metal complexes: applications in organic synthesis, *Chem. Rev.*, 2013, **113**, 5322–5363.

9. N. A. Romero and D. A. Nicewicz, Organic photoredox catalysis, *Chem. Rev.*, 2016, **116**, 10075–10166.

10. J. D. Bell and J. A. Murphy, Recent advances in visible light-activated radical coupling reactions triggered by (i) ruthenium, (ii) iridium and (iii) organic photoredox agents, *Chem. Soc. Rev.*, 2021, **50**, 9540–9685.

11. J. W. Beatty, J. J. Douglas, R. Miller, R. C. McAtee, K. P. Cole and C. R. J. Stephenson, Photochemical perfluoroalkylation with pyridine *N*-oxides: mechanistic insights and performance on a kilogram scale, *Chem*, 2016, **1**, 456–472.

12. H. G. Yayla, F. Peng, I. K. Mangion, M. McLaughlin, L.-C. Campeau, I. W. Davies, D. A. DiRocco and R. R. Knowles, Discovery and mechanistic study of a photocatalytic indoline dehydrogenation for the synthesis of elbasvir, *Chem. Sci.*, 2016, **7**, 2066–2073.

13. H. Sugihara and K. Hiratani, 1,10-Phenanthroline derivatives as ionophores for alkali metal ions, *Coord. Chem. Rev.*, 1996, **148**, 285–299.

14. A. Juris, V. Balzani, F. Barigelletti, S. Campagna, P. Belser and A. von Zelewsky, Ru(II) polypyridine complexes: photophysics, photochemistry, eletrochemistry, and chemiluminescence, *Coord. Chem. Rev.*, 1988, **84**, 85–277.

15. F. Teply, Photoredox catalysis by $[Ru(bpy)_3]^{2+}$ to trigger transformations of organic molecules. Organic synthesis using visible-light photocatalysis and its 20th century roots, *Collect. Czech. Chem. Commun.*, 2011, **76**, 859–917.
16. A. A. Yakushev, A. S. Abel, A. D. Averin, I. P. Beletskaya, A. V. Cheprakov, I. S. Ziankou, L. Bonneviot and A. Bessmertnykh-Lemeune, Visible light photocatalysis promoted by solid- and liquid-phase immobilized transition metal complexes in organic synthesis, *Coord. Chem. Rev.*, 2022, **458**, 214331.
17. A. Mitrofanov, S. Brandes, F. Herbst, S. Rigolet, A. Bessmertnykh-Lemeune and I. Beletskaya, Immobilization of copper complexes with (1,10-phenanthrolinyl)phosphonates on titania supports for sustainable catalysis, *J. Mater. Chem. A*, 2017, **5**, 12216–12235.
18. N. E. Borisova, A. V. Kharcheva, S. V. Patsaeva, L. A. Korotkov, S. Bakaev, M. D. Reshetova, K. A. Lyssenko, E. V. Belova and B. F. Myasoedov, Hard-and-soft phosphinoxide receptors for f-element binding: structure and photophysical properties of europium(III) complexes, *Dalton Trans.*, 2017, **46**, 2238–2248.
19. L. Xu, N. Pu, Y. Li, P. Wei, T. Sun, C. Xiao, J. Chen and C. Xu, Selective separation and complexation of trivalent actinide and lanthanide by a tetradentate soft–hard donor ligand: solvent extraction, spectroscopy, and DFT calculation, *Inorg. Chem.*, 2019, **58**, 4420–4430.
20. S. Amthor, P. Keil, D. Nauroozi, D. Perleth and S. Rau, Phosphonate substituent in a 1,10-phenanthroline ligand boosts light-driven catalytic water oxidation performance sensitized by ruthenium chromophores, *Eur. J. Inorg. Chem.*, 2021, **2021**, 4790–4798.
21. A. S. Abel, A. D. Averin, I. P. Beletskaya and A. Bessmertnykh-Lemeune, Transition-metal-catalyzed functionalization of 1,10-phenanthrolines and their complexes. in *Taggets in Heterocyclic Systems: Chemistry and Properties*, eds. O. A. Attanasi, B. Gabriele, P. Merino and D. Spinelli, Società Chimica Italiana, Rome, Italy, 2020, vol. 24, pp. 419–444.
22. N. Iqbal, J. Jung, S. Park and E. J. Cho, Controlled trifluoromethylation reactions of alkynes through visible-light photoredox catalysis, *Angew. Chem., Int. Ed.*, 2014, **53**, 539–542.
23. T. Chatterjee, J. Y. Cho and E. J. Cho, Synthesis of substituted oxazoles by visible-light photocatalysis, *J. Org. Chem.*, 2016, **81**, 6995–7000.
24. G.-R. Park, J. Moon and E. J. Cho, Visible-light-induced installation of oxyfluoroalkyl groups, *Chem. Commun.*, 2017, **53**, 12786–12789.

25. J. Chen, H.-M. Guo, Q.-Q. Zhao, J.-R. Chen and W.-J. Xiao, Visible light-driven photocatalytic generation of sulfonamidyl radicals for alkene hydroamination of unsaturated sulfonamides, *Chem. Commun.*, 2018, **54**, 6780–6783.
26. J. Guo, Y.-Z. Fan, Y.-L. Lu, S.-P. Zheng and C.-Y. Su, Visible-light photocatalysis of asymmetric [2+2] cycloaddition in cage-confined nanospace merging chirality with triplet-state photosensitization, *Angew. Chem., Int. Ed.*, 2020, **59**, 8661–8669.
27. G. V. Morozkov, A. S. Abel, M. A. Filatov, S. E. Nefedov, V. A. Roznyatovsky, A. V. Cheprakov, A. Y. Mitrofanov, I. S. Ziankou, A. D. Averin, I. P. Beletskaya, J. Michalak, C. Bucher, L. Bonneviot and A. Bessmertnykh-Lemeune, Ruthenium(II) complexes with phosphonate-substituted phenanthroline ligands: synthesis, characterization and use in organic photocatalysis, *Dalton Trans.*, 2022, **51**, 13612–13630.
28. I. S. Zenkov, A. A. Yakushev, A. S. Abel, A. D. Averin, A. G. Bessmertnykh-Lemeune and I. P. Beletskaya, Photocatalytic activity of ruthenium(II) complex with 1,10-phenanthroline-3,8-dicarboxylic acid in aerobic oxidation reactions, *Russ. J. Org. Chem.*, 2021, **57**, 1398–1404.
29. S. A. Trammell, J. A. Moss, J. C. Yang, B. M. Nakhle, C. A. Slate, F. Odobel, M. Sykora, B. W. Erickson and T. J. Meyer, Sensitization of TiO_2 by phosphonate-derivatized proline assemblies, *Inorg. Chem.*, 1999, **38**, 3665–3669.
30. M. Montalti, S. Wadhwa, W. Y. Kim, R. A. Kipp and R. H. Schmehl, Luminescent ruthenium(II) bipyridyl−phosphonic acid complexes: pH dependent photophysical behavior and quenching with divalent metal ions, *Inorg. Chem.*, 2000, **39**, 76–84.
31. W. J. Youngblood, S.-H. A. Lee, Y. Kobayashi, E. A. Hernandez-Pagan, P. G. Hoertz, T. A. Moore, A. L. Moore, D. Gust and T. E. Mallouk, Photoassisted overall water splitting in a visible light-absorbing dye-sensitized photoelectrochemical cell, *J. Am. Chem. Soc.*, 2009, **131**, 926–927.
32. A. M. Lapides, D. L. Ashford, K. Hanson, D. A. Torelli, J. L. Templeton and T. J. Meyer, Stabilization of a ruthenium(II) polypyridyl dye on nanocrystalline TiO_2 by an electropolymerized overlayer, *J. Am. Chem. Soc.*, 2013, **135**, 15450–15458.
33. M. R. Norris, J. J. Concepcion, Z. Fang, J. L. Templeton and T. J. Meyer, Low-overpotential water oxidation by a surface-bound ruthenium-chromophore–ruthenium-catalyst assembly, *Angew. Chem., Int. Ed.*, 2013, **52**, 13580–13583.
34. D. M. Ryan, M. K. Coggins, J. J. Concepcion, D. L. Ashford, Z. Fang, L. Alibabaei, D. Ma, T. J. Meyer and M. L. Waters, Synthesis and electrocatalytic water oxidation by

electrode-bound helical peptide chromophore–catalyst assemblies, *Inorg. Chem.*, 2014, **53**, 8120–8128.

35. H. Luo, Z. Fang, N. Song, T. Garvey, R. Lopez and T. J. Meyer, High surface area antimony-doped tin oxide electrodes templated by graft copolymerization. applications in electrochemical and photoelectrochemical catalysis, *ACS Appl. Mater. Interfaces*, 2015, **7**, 25121–25128.
36. D. L. Ashford, M. K. Brennaman, R. J. Brown, S. Keinan, J. J. Concepcion, J. M. Papanikolas, J. L. Templeton and T. J. Meyer, Varying the electronic structure of surface-bound ruthenium(II) polypyridyl complexes, *Inorg. Chem.*, 2015, **54**, 460–469.
37. S. L. Esarey and B. M. Bartlett, pH-Dependence of binding constants and desorption rates of phosphonate- and hydroxamate-anchored $[Ru(bpy)_3]^{2+}$ on TiO_2 and WO_3, *Langmuir*, 2018, **34**, 4535–4547.
38. I. Purnama, Y. Kubo and J. Y. Mulyana, A robust ruthenium complex with nonyl-substituted bpy ligand for dye-sensitized photoelectrochemical cell application, *Inorg. Chim. Acta*, 2018, **471**, 467–474.
39. L. Troian-Gautier, B. N. DiMarco, R. N. Sampaio, S. L. Marquard and G. J. Meyer, Evidence that $\Delta S^{\ddagger}$ controls interfacial electron transfer dynamics from anatase TiO_2 to molecular acceptors, *J. Am. Chem. Soc.*, 2018, **140**, 3019–3029.
40. V. K. Davis, R. N. Sampaio, S. L. Marquard and G. J. Meyer, Electric fields detected on dye-sensitized TiO_2 interfaces: influence of electrolyte composition and ruthenium polypyridyl anchoring group type, *J. Phys. Chem. C*, 2018, **122**, 12712–12722.
41. M. D. Brady, L. Troian-Gautier, R. N. Sampaio, T. C. Motley and G. J. Meyer, Optimization of photocatalyst excited- and ground-state reduction potentials for dye-sensitized hbr splitting, *ACS Appl. Mater. Interfaces*, 2018, **10**, 31312–31323.
42. I. Purnama, Salmahaminati, M. Abe, M. Hada, Y. Kubo and J. Y. Mulyana, Factors influencing the photoelectrochemical device performance sensitized by ruthenium polypyridyl dyes, *Dalton Trans.*, 2019, **48**, 688–695.
43. M. M. Raber, M. D. Brady, L. Troian-Gautier, J. C. Dickenson, S. L. Marquard, J. T. Hyde, S. J. Lopez, G. J. Meyer, T. J. Meyer and D. P. Harrison, Fundamental factors impacting the stability of phosphonate-derivatized ruthenium polypyridyl sensitizers adsorbed on metal oxide surfaces, *ACS Appl. Mater. Interfaces*, 2018, **10**, 22821–22833.
44. A. Zaban, S. Ferrere and B. A. Gregg, Relative energetics at the semiconductor/sensitizing dye/electrolyte interface, *J. Phys. Chem. B*, 1998, **102**, 452–460.

45. K. Neuthe, F. Bittner, F. Stiemke, B. Ziem, J. Du, M. Zellner, M. Wark, T. Schubert and R. Haag, Phosphonic acid anchored ruthenium complexes for ZnO-based dye-sensitized solar cells, *Dyes Pigm.*, 2014, **104**, 24–33.
46. I. Gillaizeau-Gauthier, F. Odobel, M. Alebbi, R. Argazzi, E. Costa, C. A. Bignozzi, P. Qu and G. J. Meyer, Phosphonate-based bipyridine dyes for stable photovoltaic devices, *Inorg. Chem.*, 2001, **40**, 6073–6079.
47. M. R. Norris, J. J. Concepcion, C. R. K. Glasson, Z. Fang, A. M. Lapides, D. L. Ashford, J. L. Templeton and T. J. Meyer, Synthesis of phosphonic acid derivatized bipyridine ligands and their ruthenium complexes, *Inorg. Chem.*, 2013, **52**, 12492–12501.
48. H. Zabri, I. Gillaizeau, C. A. Bignozzi, S. Caramori, M.-F. Charlot, J. Cano-Boquera and F. Odobel, Synthesis and comprehensive characterizations of new *cis*-RuL_2X_2 (X = Cl, CN, and NCS) sensitizers for nanocrystalline TiO_2 solar cell using bis-phosphonated bipyridine ligands (L), *Inorg. Chem.*, 2003, **42**, 6655–6666.
49. E. Kowalska, K. Yoshiiri, Z. Wei, S. Zheng, E. Kastl, H. Remita, B. Ohtani and S. Rau, Hybrid photocatalysts composed of titania modified with plasmonic nanoparticles and ruthenium complexes for decomposition of organic compounds, *Appl. Catal., B*, 2015, **178**, 133–143.
50. M. D. Brady, R. N. Sampaio, D. Wang, T. J. Meyer and G. J. Meyer, Dye-sensitized hydrobromic acid splitting for hydrogen solar fuel production, *J. Am. Chem. Soc.*, 2017, **139**, 15612–15615.
51. M. S. Eberhart, L. M. R. Bowers, B. Shan, L. Troian-Gautier, M. K. Brennaman, J. M. Papanikolas and T. J. Meyer, Completing a charge transport chain for artificial photosynthesis, *J. Am. Chem. Soc.*, 2018, **140**, 9823–9826.
52. Y. Y. Enakieva, M. V. Volostnykh, S. E. Nefedov, G. A. Kirakosyan, Y. G. Gorbunova, A. Y. Tsivadze, A. G. Bessmertnykh-Lemeune, C. Stern and R. Guilard, Gallium(III) and indium(III) complexes with *meso*-monophosphorylated porphyrins: synthesis and structure. a first example of dimers formed by the self-assembly of *meso*-porphyrinylphosphonic acid monoester, *Inorg. Chem.*, 2017, **56**, 3055–3070.
53. K. R. Bargawi, A. Llobet and T. J. Meyer, Synthetic design of MLCT excited states. Ligand-substituted, mono-2,2'-bipyridine complexes of ruthenium(II), *J. Am. Chem. Soc.*, 1988, **110**, 7751–7759.

54. H. N. K. Herath, A. L. MacRae, A. Ugrinov, G. R. Morello and A. R. Parent, Electrochemical properties of Ru polypyridyl phosphonates, *Eur. J. Inorg. Chem.*, 2023, **26**, e202200747.

55. D. S. Eggleston, K. A. Goldsby, D. J. Hodgson and T. J. Meyer, Crystal and molecular structures of *cis*-$[Ru(bpy)_2Cl_2]\cdot 3.5H_2O$ and *cis*-$[Ru(bpy)_2Cl_2]Cl\cdot 2H_2O$, *Inorg. Chem.*, 1985, **24**, 4573–4580.

56. S. S. Bhat, A. S. Kumbhar, P. Lönnecke and E. Hey-Hawkins, Self-association of ruthenium(II) polypyridyl complexes and their interactions with calf thymus DNA, *Inorg. Chem.*, 2010, **49**, 4843–4853.

57. B.-H. Ye, L.-N. Ji, F. Xue and T. C. W. Mak, Synthesis, characterization and crystal structure of ruthenium(II) polypyridyl complexes, *Transition Met. Chem.*, 1999, **24**, 8–12.

58. X. Yang, M. Kritikos, B. Åkermark and L. Sun, Axial ligand exchange reaction on ruthenium phthalocyanines, *J. Porphyrins Phthalocyanines*, 2005, **09**, 248–255.

59. K. Nakamaru, Luminescence quantum yields, and lifetimes of trischelated ruthenium(II) mixed-ligand complexes including 3,3′-dimethyl-2,2′-bipyridyl, *Bull. Chem. Soc. Jpn.*, 1982, **55**, 2697–2705.

60. H. Ishida, S. Tobita, Y. Hasegawa, R. Katoh and K. Nozaki, Recent advances in instrumentation for absolute emission quantum yield measurements, *Coord. Chem. Rev.*, 2010, **254**, 2449–2458.

61. V. Balzani, A. Juris, M. Venturi, S. Campagna and S. Serroni, Luminescent and redox-active polynuclear transition metal complexes, *Chem. Rev.*, 1996, **96**, 759–834.

62. H. M. L. Davies and D. Morton, Recent advances in C–H functionalization, *J. Org. Chem.*, 2016, **81**, 343–350.

63. N. Holmberg-Douglas and D. A. Nicewicz, Photoredox-catalyzed C–H functionalization reactions, *Chem. Rev.*, 2022, **122**, 1925–2016.

64. L. Shi and W. Xia, Photoredox functionalization of C–H bonds adjacent to a nitrogen atom, *Chem. Soc. Rev.*, 2012, **41**, 7687–7697.

65. H. Bartling, A. Eisenhofer, B. König and R. M. Gschwind, The photocatalyzed aza-Henry reaction of *N*-aryltetrahydroisoquinolines: comprehensive mechanism, $h^{\bullet}$- versus h^{+}-abstraction, and background reactions, *J. Am. Chem. Soc.*, 2016, **138**, 11860–11871.

66. Z. Mahmood, J. He, S. Cai, Z. Yuan, H. Liang, Q. Chen, Y. Huo, B. König and S. Ji, Tuning the photocatalytic performance of ruthenium(II) polypyridine complexes via ligand

modification for visible-light-induced phosphorylation of tertiary aliphatic amines, *Chem. – Eur. J.*, 2023, **29**, e202202677.

67. A. G. Condie, J. C. González-Gómez and C. R. J. Stephenson, Visible-light photoredox catalysis: aza-Henry reactions *via* C−H functionalization, *J. Am. Chem. Soc.*, 2010, **132**, 1464–1465.
68. M. Rueping, S. Zhu and R. M. Koenigs, Photoredox catalyzed C–P bond forming reactions—visible light mediated oxidative phosphonylations of amines, *Chem. Commun.*, 2011, **47**, 8679–8681.
69. W. Xie, N. Liu, B. Gong, S. Ning, X. Che, L. Cui and J. Xiang, Electrochemical cross-dehydrogenative coupling of *N*-aryl-tetrahydroisoquinolines with phosphites and indole, *Eur. J. Org. Chem.*, 2019, **2019**, 2498–2501.
70. Y.-X. Tan, S.-X. Lin, C. Liu, Y. Huang, M. Zhou, Q. Kang, D. Yuan and M. Hong, Boosting photocatalytic cross-dehydrogenative coupling reaction by incorporating $[Ru^{II}(bpy)_3]$ into a radical metal-organic framework, *Appl. Catal., B*, 2018, **227**, 425–432.
71. M. Rueping, S. Zhu and R. M. Koenigs, Visible-light photoredox catalyzed oxidative Strecker reaction, *Chem. Commun.*, 2011, **47**, 12709–12711.
72. A. Mitrofanov, A. Bessmertnykh-Lemeune, C. Stern, R. Guilard, N. Gulyukina and I. Beletskaya, Palladium-catalyzed synthesis of mono- and diphosphorylated 1,10-phenanthrolines, *Synthesis*, 2012, **44**, 3805–3810.
73. P. A. Lay, A. M. Sargeson, H. Taube, M. H. Chou and C. Creutz, *cis*-Bis(2,2′-bipyridine-*N*,*N*′) complexes of ruthenium(III)/(II) and osmium(III)/(II), *Inorg. Synth.*, 1986, **24**, 291–299.
74. J.-X. Jiang, Y. Li, X. Wu, J. Xiao, D. J. Adams and A. I. Cooper, Conjugated microporous polymers with rose bengal dye for highly efficient heterogeneous organo-photocatalysis, *Macromolecules*, 2013, **46**, 8779–8783.
75. I. Martín-García and F. Alonso, Synthesis of dihydroindoloisoquinolines through copper-catalyzed cross-dehydrogenative coupling of tetrahydroisoquinolines and nitroalkanes, *Chem. – Eur. J.*, 2018, **24**, 18857–18862.
76. M. Taniguchi, J. S. Lindsey, D. F. Bocian and D. Holten, Comprehensive review of photophysical parameters (ε, Φ^f, τ_s) of tetraphenylporphyrin (H_2TPP) and zinc tetraphenylporphyrin (ZnTPP) – Critical benchmark molecules in photochemistry and photosynthesis, *J. Photochem. Photobiol., C*, 2021, **46**, 100401.

77. Sheldrick, G. A short history of SHELX, *Acta Crystallogr., Sect. A: Found. Crystallogr.* **2008,** *64*, 112–122.

78. A. Spek, PLATON SQUEEZE: a tool for the calculation of the disordered solvent contribution to the calculated structure factors, *Acta Crystallogr. Sect. C: Struct. Chem.*, 2015, **71**, 9–18.

79. Q. Liu, Y.-N. Li, H.-H. Zhang, B. Chen, C.-H. Tung and L.-Z. Wu, Reactivity and mechanistic insight into visible-light-induced aerobic cross-dehydrogenative coupling reaction by organophotocatalysts, *Chem. – Eur. J.*, 2012, **18**, 620–627.

80. T. Thatikonda, S. K. Deepake and U. Das, *α*-Angelica lactone in a new role: facile access to *N*-aryl tetrahydroisoquinolinones and isoindolinones *via* organocatalytic *α*-CH_2 oxygenation, *Org. Lett.*, 2019, **21**, 2532–2535.

81. S.-I. Murahashi, N. Komiya, H. Terai and T. Nakae, Aerobic ruthenium-catalyzed oxidative cyanation of tertiary amines with sodium cyanide, *J. Am. Chem. Soc.*, 2003, **125**, 15312–15313.

82. P. Kumar, S. Varma and S. L. Jain, A TiO_2 immobilized Ru(II) polyazine complex: a visible-light active photoredox catalyst for oxidative cyanation of tertiary amines, *J. Mater. Chem. A*, 2014, **2**, 4514–4519.